this possibility with a few calculations.[42] The data in Figure 9 predict a temperature jump of ca. 64 °C, while the complete laser power used can account for only a maximum of ca. 6 °C. The closed-shell anions clearly must be generated by a photochemical event, and we suggest the cleavage of the radical ion pair.

Conclusions

A series of molecules each composed of a stable carbanion and carbocation, covalently attached to each other, has been photolysed and studied via picosecond and nanosecond laser techniques. These molecules undergo a sequence of events that begins with absorption of a photon by one of two localized chromophores in each precursor (i.e., the stilbene of TPCP or the aryl portion of the starting carbanion). The constraints of the geometry in the molecules prevent overlap of the π-systems, a result confirmed by the absence of any EDA bands in the UV-visible spectrum and from the fluorescence data. The singlet excited states initiate an electron-transfer event at rates that were too fast to measure under the conditions employed. In other words, the radical ions were observed within the shortest measurement time scale (< ca. 25 ps). The radical ion pairs have two possible alternatives: (1) back electron transfer to form the triplet of the triphenylcyclopropenyl part and (2) bond fragmentation of the central bond (i.e., the one connecting the carbanion to the carbocation). Apparently, the presence of ions from the latter cleavage depends on the relative rates of the two processes. The ions are only observed in those cases where the bond breakage can compete with the back electron transfer. The fragmentation of the radical ion pair can, in principle, give either the ion or radical pair. For the examples in this study, the ions are favored thermodynamically over the radicals, a result that can be predicted (or confirmed) from the redox properties of the ions (i.e., available from electrochemical data). We suggest that the intramolecular radical ion pair is both a novel and a general method for fragmentation of carbon-carbon bonds. We are exploring other systems in which the fragmentation process is greatly enhanced and in which neutral radicals are the ultimate products.

Acknowledgment. We acknowledge the support of the NSF (KSP and EDO) and the Gas Research Institute (EMA and KEM). We are thankful to Steve Angel (Colorado) for measuring picosecond decay kinetics and for discussions concerning kinetic schemes, to Ed Hilinski (Florida State) for suggestions concerning solvent effects on electron-transfer reactions and stilbene cyclization, to T. J. Meyer (North Carolina) for the use of the nanosecond apparatus, and to Earl Danielson and Wayne Jones (UNC) for comments concerning its operation. N.J.P. acknowledges the University of Arkansas and the Department of Chemistry & Biochemistry for a sabbatical leave and Boulder Memorial Hospital for making its completion a possibility.

(42) At 25 °C, 2 mM TPCP-NMN in acetonitrile that contains 40 mM $TPCP^+BF_4^-$ will produce 6.5 μM NMN^- (K_{hetero} = 1.35 × 10^{-4}; ref 1c). At the earliest times recorded in Figure 8, the OD change of 0.05 for NMN^- accounts for an additional 1.7 μM NMN^- (molar absorptivity 3.01 × 10^{-4}; ref 1c). An apparent new K can be determined (from [$TPCP^+$] = 40 mM, [NMN^-] = 8.2 μM, and [TPCP-NMN] = 1.99 mM] and is found to be K_{app} = 1.65 × 10^{-4}. For this to be true under thermal conditions, the new temperature should be 89 °C, representing a rise of 64 °C. If we assume an irradiated volume 1 cm long and 0.5 cm in diameter (ca. 63 μL or 1.2 μmol of acetonitrile), a laser pulse of 20 mJ (20% of the maximum possible output at 355 nm, amplifier at 50% and oscillator at 50%), and a heat capacity of 0.7 cal/mol deg, we predict a temperature jump of ca. 6 °C if all of the laser power becomes heat!

Rare α-Alkyl Isomers of Cobalamins: Synthesis, Characterization, and Properties of Two Diastereomers of the α-Alkylcobalamin, α-(2-Oxo-1,3-dioxolan-4-yl)cobalamin

Yun W. Alelyunas,[†] Paul E. Fleming,[†] Richard G. Finke,*[,†] Thomas G. Pagano,[‡] and Luigi G. Marzilli[‡]

Contribution from the Department of Chemistry, University of Oregon, Eugene, Oregon 97403, and Department of Chemistry, Emory University, Atlanta, Georgia 30322.
Received September 10, 1990

Abstract: The synthesis, characterization, 2-D NMR (HOHAHA, NOESY, HMQC, and HMBC spectroscopies), and reactivities of a new α-alkylcobalamin are described (an α-alkylcobalamin has the axial alkyl group attached to the cobalt from the "bottom" or α face of the corrin ring). The α-alkylcobalamin, α-(2-oxo-1,3-dioxolan-4-yl)cobalamin (**1**), is the first example of an α-alkylcobalamin with a secondary alkyl group and the first case with a chiral alkyl group (i.e., where α-alkylcobalamin diastereomers are produced). It is also the first α-alkylcobalamin completely characterized (HPLC, UV-visible, IR, FAB-MS, and 1- and 2-D NMR methods). Anaerobic photolysis converts **1** to its β isomer, β-(2-oxo-1,3-dioxolan-4-yl)cobalamin (**2**), where the alkyl group is now attached to the cobalt from the usual, β or "top" side of the corrin. Physical properties previously unavailable for any α-alkylcobalamin were measured for **1**, notably the β-side axial base binding constants [for 1-methylimidazole, pyridine, (±)-histidine, and 1,5,6-trimethylbenzimidazole], and the thermal stability of the individual diastereomers of **1**. Possible mechanisms for, and the factors controlling, the formation of α- and β-alkylcobalamins are presented and discussed.

Introduction

The two outstanding examples of a β-alkylcobalamin are β-(5'-deoxyadenosyl)cobalamin (coenzyme B_{12}) and β-methylcobalamin, the β prefix indicating (as usual) that the alkyl group attached to cobalt is on the "upper" face of the structure as shown in Figure 1A for β-methylcobalamin. α-Alkylcobalamins, on the other hand (Figure 1B), are relatively rare and thus little studied; established examples are limited to α-cyanocobalamin,[1-3] α-me-

[†] University of Oregon.
[‡] Emory University.

(1) Work by Friedrich and co-workers provided the discovery and pioneering studies of α-alkylcorrins.[4-7,8b]

0002-7863/91/1513-3781$02.50/0

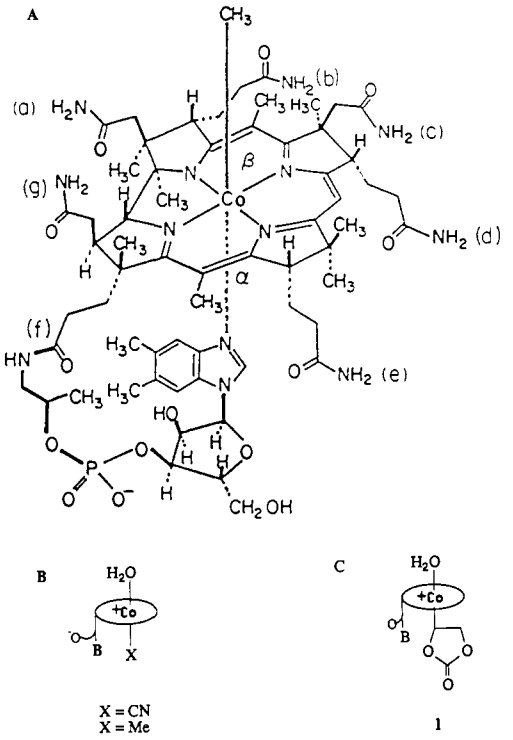

Figure 1. (A) Structure and numbering scheme for methylcobalamin. (B) Abbreviated structural representation for α-cyano- (X = CN) and α-methyl- (X = Me) cobalamin. (C) Abbreviated structural representation for **1**.

thylcobalamin,[4-7] and Brown's recent communication describing α-CF_3CH_2-cobalamin[8a] (a few α-alkyl*cobinamides* are also known).[8,9] α-Alkylcobalamins with sterically bulky secondary alkyl groups were unknown[10-12] until the present work, and even for α-methylcobalamin our understanding of its properties is limited by the fact that it is characterized only by structurally indirect methods (chromatography and UV–visible spectroscopy). Moreover, virtually nothing is known about the detailed mechanisms of the reactions leading to α- and β-alkylcobalamins and the factors that affect the α/β ratio. For example, the steric and electronic factors favoring or disfavoring α-cobalamins are unclear, although the example of X = CN^- (Figure 1B) suggests that small groups that are electron withdrawing relative to CH_3 may favor α-cobalamin isomers. Overall, little is known about how one might develop general, regiospecific syntheses leading to pure α-cobalamins.

Scheme I

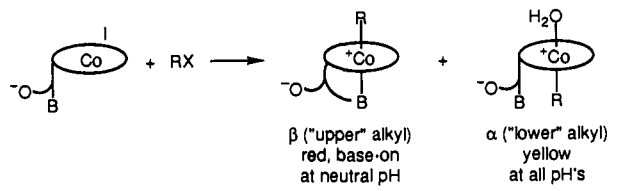

The biological relevance, *if any*, of α-alkylcobalamins is probably limited to α-methylcobalamin. Recent model studies of cobalamin-dependent methyl transferase led to the suggestion that an α-methylcorrin *may* be an active intermediate in such enzymes.[13] Clearly, the α isomers of alkylcobalamins merit additional study, both for their fundamental chemistry and for their possible role in biology.

Herein we report the synthesis, characterization, and properties of the α-alkylcobalamin, α-(2-oxo-1,3-dioxolan-4-yl)cobalamin, (**1**; Figure 1C), in which the alkyl group is a relatively bulky and electron-withdrawing five-membered, 1,3-dioxolan-4-yl ring. The α-alkylcobalamin **1** is also the first example with a chiral carbon attached to cobalt and thus the first case where α-cobalamin diastereomers are possible, are in fact observed, and have been isolated in pure form.

Results and Discussion

General Synthetic Routes to α- and β-Alkylcobalamins. Alkylcobalamins are generally synthesized from the reduction of hydroxocobalamin (Co^{III}-B_{12a}) or cyanocobalamin with reducing reagents such as Zn (as a slurry in acidic solution) or $NaBH_4$ (in neutral or basic solution).[14a] Oxidative addition of an alkyl halide to the resultant H^+·Co^I-B_{12s} or Co^I-B_{12s} then produces the desired alkylcobalamin. Since the Co^I-B_{12s} exists in its base-off form[14b-d] (i.e., with the benzimidazole base not coordinated to cobalt), the alkyl group should in principle attach to the cobalt from *both* the β and the α faces of the corrin (Scheme I). So far, however, only β-alkylcobalamin isomers are *isolated* from almost all known alkylcobalamin syntheses (although the present work and Brown's recent results[8a] suggest that α isomers may be much more common than previously thought).[15]

Synthesis of α-(2-Oxo-1,3-dioxolan-4-yl)cobalamin (1) Initially as Its Mixture of Two Diastereomers. Our interest in the mechanism for the rearrangement step of the diol dehydratase reaction has led to the synthesis of the carbonate-protected form of (dihydroxyethyl)cobalamin, one putative intermediate in the widely debated cobalt-participation mechanism.[16] The synthesis

(2) α and β isomers of cyanocobinamide: Needham, T. E.; Matwiyoff, N. A.; Walker, T. E.; Hogenkamp, H. P. C. *J. Am. Chem. Soc.* **1973**, *95*, 5019–5024.

(3) (a) α and β isomers of cyanocobinamide: Brown, K. L.; Hakimi, J. M. *Inorg. Chem.* **1984**, *23*, 1756–1764. (b) Reenstra, W. W.; Jencks, W. P. *J. Am. Chem. Soc.* **1979**, *101*, 5780–5791.

(4) Friedrich, W.; Nordmeyer, J. P. *Z. Naturforsch.* **1968**, *23B*, 1119–1120.

(5) Friedrich, W.; Nordmeyer, J. P. *Z. Naturforsch.* **1969**, *24B*, 588–596.

(6) Moskophidis, M.; Klotz, C. M.; Friedrich, W. *Z. Naturforsch.* **1976**, *31C*, 255–262.

(7) Moskophidis, M. In *Vitamin B_{12}*; Zagalak, B., Friedrich, W. Eds.; deGruyter: Berlin, FRG, 1979; pp 189–192.

(8) (a) Brown, K. L.; Evans, D. R. *Inorg. Chem.* **1990**, *29*, 2561. We thank Professor Brown for his comments on the present article and for informing us that additional examples of α-alkylcobalamins and -cobinamides (R = CH_3, CHF_2, CF_3, $NCCH_2$, and $EtOCH_2CH_2$) will be forthcoming from his laboratories. (b) α and β isomers of methylcobinamide: Friedrich, W.; Messerschmidt, R. *Z. Naturforsch.* **1969**, *24B*, 465–467. Friedrich, W.; Moskophidis, M. *Z. Naturforsch.* **1970**, *25B*, 979.

(9) α and β isomers of ethynylcobinamide: Baldwin, D. A.; Betterton, E. A.; Pratt, J. M. *J. Chem. Soc., Dalton Trans.* **1983**, 225–229.

(10) The reported synthesis of what is very likely the α isomer of acetylcobalamin (as Pratt has previously suggested),[12] using Zn/HOAc and acetic acid anhydride as the acetylation reagent, produced an acetylcobalamin exhibiting a base-off-like spectrum at all pH's.[11] Unfortunately, the resultant acetylcobalamin was not characterized further.

(11) Smith, E. L.; Mervyn, L.; Muggleton, P. W.; Johnson, A. W.; Shaw, N. *Ann. N.Y. Acad. Sci.* **1964**, *112*, 565, and references cited therein.

(12) Pratt, J. M. *Inorganic Chemistry of Vitamin B_{12}*, Academic Press: London, 1970; p 119.

(13) See Scheme II in: Fanchiang, Y.-T.; Bratt, G. T.; Hogenkamp, H. P. C. *Proc. Natl. Acad. Sci. U.S.A.* **1984**, *81*, 2698. However, the minimal evidence and questionable argument therein against a S_E2 mechanism, and the thermochemically ca. 0.6-V uphill and thus improbable disproportionation mechanism proposed instead, $MeCo^{III} + Co^{III} \rightleftharpoons MeCo^{IV} + Co^{II}$, require reinvestigation.

(14) (a) Dolphin, D. In *Methods in Enzymology*; Academic Press, New York, 1971; Vol. XVIII, p 34. (b) Rubinson, K. A.; Parekh, H. V.; Itabashi, E.; Mark, H. B., Jr. *Inorg. Chem.* **1983**, *22*, 458. (c) Lexa, D.; Saveant, J. M. *J. Am. Chem. Soc.* **1976**, *98*, 2652. (d) Brodie, J. D.; Poe, M. *Biochemistry*, **1971**, *10*, 914.

(15) (a) The present study suggests that many of the earlier syntheses of alkylcobalamins with electron-withdrawing groups such as acetyl, ethynyl, carboxymethyl, vinyl, and (carboxycarbonyl)methyl should produce at least some α isomers,[14a,15b] but the detection of these isomers may have been missed since (carboxymethyl)cellulose columns were employed in their workups (the α isomer **1**·H^+ in the present work sticks to such a column and cannot be eluted by H_2O). (b) The low (37%) yield reported in the recent synthesis of (methoxycarbonyl)methylcobalamin also suggests that the α isomer is a reaction product: Timebart, O.; Walder, L.; Scheffold, R. *Ber. Bunsenges. Phys. Chem.* **1988**, *92*, 1225–1231.

(16) (a) Wang, Y.; Finke, R. G. *Inorg. Chem.* **1989**, *28*, 983. (b) Wang, Y. Ph.D. Thesis, University of Oregon, 1988. (c) Alelyunas, Y. W.; Finke, R. G., manuscript in preparation. (d) Earlier control experiments (see ref 16b, 64–67 and 227), done to optimize the yield of β-**2**, were chosen as good initial guesses for the optimum conditions for the synthesis of **1**. Those controls demonstrate that reaction times longer than 10–15 min lead to Zn reductive cleavage of **2**'s Co–C bond and to a side reaction between Zn and chloroethylene carbonate.

Scheme II

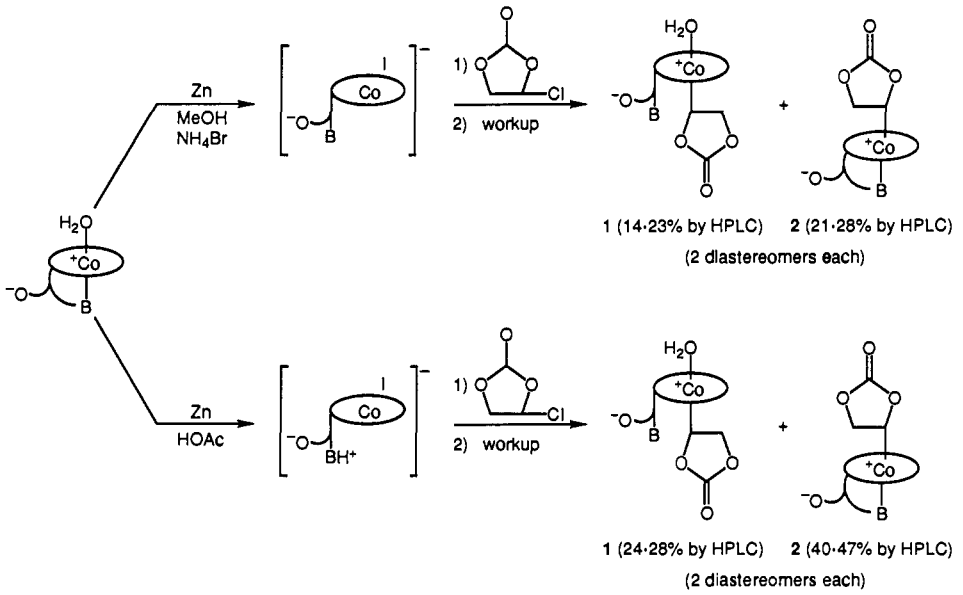

of **1** was achieved by using a slurry of Zn as reducing reagent both in $MeOH/NH_4^+Br^-$ in early experiments (HPLC yields prior to workup are 14–23%) and then later in glacial acetic acid as shown in Scheme II; the most reproducible yield (24–28% by HPLC) and α/β ratio (0.6 ± 0.1) were obtained in HOAc as detailed in the Experimental Section. The variable yields in MeOH are consistent with the literature, Schrauzer and Grate having previously reported that the Zn/HOAc method is preferred for secondary alkyl halides (in MeOH, they found that secondary RX gave mostly olefins when treated with Co^I-B_{12s}).[17b] Note that **1** should (and does) exist as two diastereomers as previously found for **2**, since the cobalt corrin in B_{12} is chiral and the chloroethylene carbonate employed is racemic. (Preparative HPLC separation of **1** into its two diastereomers, α_1-**1** and α_2-**1**, will be described in a later section.) HPLC of the crude reaction mixture shows some unchanged Co^{III}-B_{12a} starting material plus two different alkylcobalamin peaks (the α-**1** and β-**2** isomers, vide infra) in a 0.6 ± 0.1 molar ratio (for the Zn/HOAc synthesis).

Workup in the case of the $Zn/MeOH/NH_4^+Br^-$ synthesis was achieved as follows. The crude product mixture containing both the α- and β-alkyls is treated with phosphate buffer to yield a pH 5.2 solution and a mixture that should be predominantly $\mathbf{1}\cdot H^+$ (5,6-dimethylbenzimidazole base-protonated **1** whose pK_a is 5.4; vide infra) and unprotonated **2** (since **2**'s protonated 5,6-dimethylbenzimidazole base pK_a is 2.2 ± 0.1).[16b] The mixture is then desalted via an XAD-2 column and the filtrate concentrated, dissolved in deionized water, and then loaded onto a cation-exchange column. The β-alkylcobalamin, **2** (also a mixture of two diastereomers), elutes first (distilled H_2O eluent), and we previously identified it unequivocally as the β-alkyl isomer.[16a,b] The α-alkylcobalamin $\mathbf{1}\cdot H^+$ sticks to (carboxymethyl)cellulose cation-exchange column and is not readily eluted by distilled H_2O (as monitored by UV–visible spectroscopy) from a Sephadex-SP cation-exchange column. However, when the eluent was changed to 0.1 or 0.2 N NaCl, the yellow α-alkylcobalamin, $\mathbf{1}\cdot H^+$ and/or **1**, (as a mixture of its two diastereomers) is separated from any Co^{III}-aquocobalamin side product that remains on the column. Following desalting on a XAD-2 column (H_2O, then 50% H_2O/50% CH_3CN eluents), *unprotonated* **1** (by ^1H NMR) is isolated without further steps as a pure, orange-red powder in 17% yield for this $Zn/MeOH/NH_4Br$ reduction method.

The Zn/HOAc preparations were worked up directly by preparative HPLC. An ether precipitation of the crude reaction mixture yielded a mixture containing $\mathbf{1}\cdot H^+$ and **2**. Preparative HPLC workup yielded *unprotonated* **1** directly in 24–28% HPLC yield (see the Experimental Section for further details).

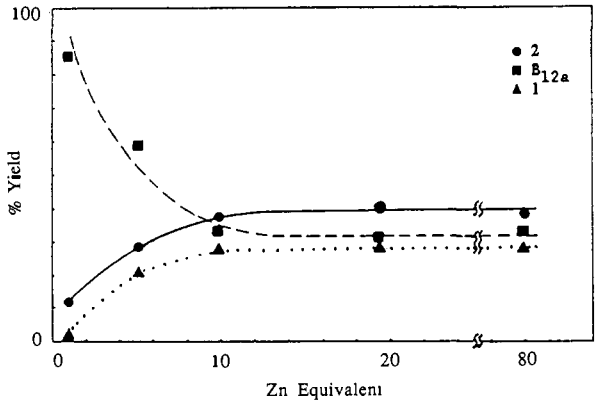

Figure 2. Plot of the percent yield of **1**, **2**, and B_{12a} vs equivalents of Zn at short, 10–15-min reaction times where Zn reductive cleavage of the Co–C bond in **1** and **2** is minimized. The percent yield is calculated from integration of the HPLC peak areas (at 280 nm where the extinction coefficients for **1**, **2**, and B_{12a} are equal within experimental error). The yields vary somewhat depending on the exact experimental conditions as documented in the Experimental Section.

Since Zn has been reported to cause reductive cleavage of Co–C bonds,[17] and since we have observed this reaction for **2** plus Zn if reaction times are not limited to 10–15 min,[16a,b,d] a control experiment with Zn/HOAc was done to check whether or not the yield or the α-**1** to β-**2** isomer distribution in the product is sensitive to the amount of Zn (i.e., to the total Zn surface area; the total reaction time was kept constant, 10–15 min). The results, Figure 2, show that the ratio of β-**2** to α-**1** is unchanged as the total Zn surface area is increased. However, the yield of both **1** and **2** *increased*, and the remaining B_{12a} starting material decreased (from 85% to 30% B_{12a} remaining with 1 vs 10 equiv of Zn, respectively), with the increase (and concomitant decrease in B_{12a}) reaching its limit at 10 equiv of Zn. These results (Figure 2) demonstrate that conditions chosen for the synthesis of **1** (i.e., those based on our earlier studies optimizing the synthesis of **2**)[16d] are in fact near optimum.

Characterization of 1. Initially **1** was characterized as its mixture of two diastereomers by HPLC, FAB-MS, UV–visible, FT-IR, and 1-D ^1H NMR spectroscopy; after we were certain it was the correct compound, then the effort needed to separate **1** into its two diastereomers was invested. HPLC of isolated, diastereomeric **1** demonstrates that it is >97% of a single corrin type. The FAB-MS of **1** exhibits a molecular ion peak of *m/e*

(17) (a) Grate, J. H.; Grate, J. W.; Schrauzer, G. N. *J. Am. Chem. Soc.* **1982**, *104*, 1588. (b) Grate, J. H.; Schrauzer, G. N. *J. Am. Chem. Soc.* **1979**, *101*, 4601.

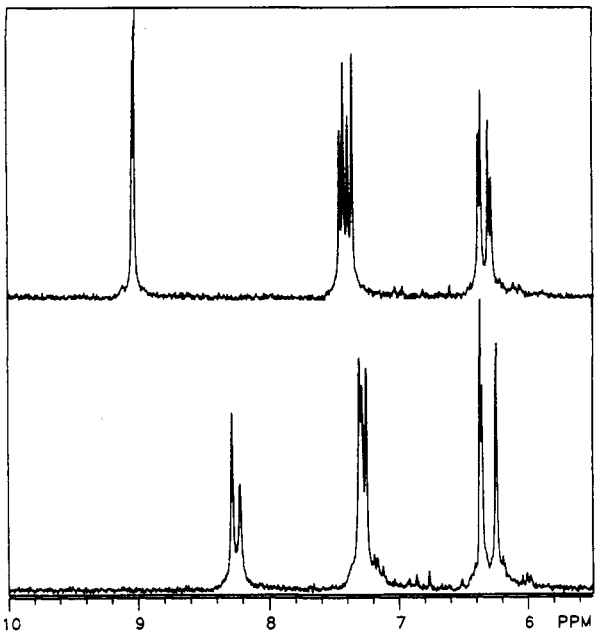

Figure 3. 300-MHz ^{1}H NMR spectroscopy. Upper: in 0.7 M DCl (D_2O). Lower: in neutral D_2O. For ease of comparison, only the downfield region from 5.5 to 10 ppm is shown here. Peak chemical shift values are given in the Experimental Section. For the complete spectrum of **1** in D_2O, see Figure H, supplementary material.

= 1416.7, consistent with the expected molecular formula of $C_{65}H_{91}O_{17}N_{13}PCo{\cdot}H^+$ [MW = 1416.58, hence no β-axial ligand such as H_2O is present (in the gas-phase FAB-MS)].[18] The FAB-MS of **1** is also identical with **2** (Figure A, supplementary material), demonstrating unequivocally that **1** and **2** are isomers.

FT-IR spectroscopy is the most direct means of characterizing the ethylene carbonate alkyl moiety in **1**. Two solvent-sensitive, characteristic peaks (due to Fermi resonance)[19] of the ethylene carbonate alkyl group are seen, 1800 and 1776 cm^{-1} in MeOH (Figure B, supplementary material). These two peaks are identical in their location and (solvent-sensitive)[19] relative intensity to the two analogous IR peaks seen for **2**.

Before examining the 2-D NMR results in detail, it is useful to summarize the key evidence unequivocally proving that **1** is an α-alkylcobalamin. This evidence is clear-cut and 8-fold: (1) **1** has the same molecular weight (by FAB-MS) as **2**, but is unequivocally not **2** (by its different HPLC retention time or ^{1}H NMR, for example); that is, **1** must be an isomer of **2**; (2) the electronic spectra as well as the 1-D ^{1}H NMR results (vide infra) show that **1** is an alkylcobalamin; yet (3) the 2-D ^{1}H NMR data demonstrate that the ethylene carbonate moiety in **1** is close in space to the benzimidazole base, which in turn is *known to be appended to the α face of the corrin*, and to the C20 methyl group, which is *known to point down on the α face*; (4) the visible spectrum of **1** in deionized H_2O (λ_{max} = 484, 324 nm; shoulder at 354 nm) in comparison to base-off β-**2** (λ_{max} = 458, 321 nm; Figure C, supplementary material) shows that the spectrum for **1** is overall "base-off"-like, but with the 484-nm band having been red-shifted by ~26 nm, *the same magnitude as observed in α-methylcobalamin* (28 nm);[9] (5) the ^{1}H and ^{13}C NMR shifts of certain key protons and carbons in **1** are more similar to those for *base-off* cobalamins and α-ribazole phosphate than to base-on cobalamins. That is, the chemical shifts of **1** confirm that it is a base-*off* alkylcobalamin even in its unprotonated form; (6) **1** exists as a base-on alkylcobalamin under all circumstances and pH conditions [pH 1 (0.1 N HCl), pH 7 buffer, and pH 10 buffer

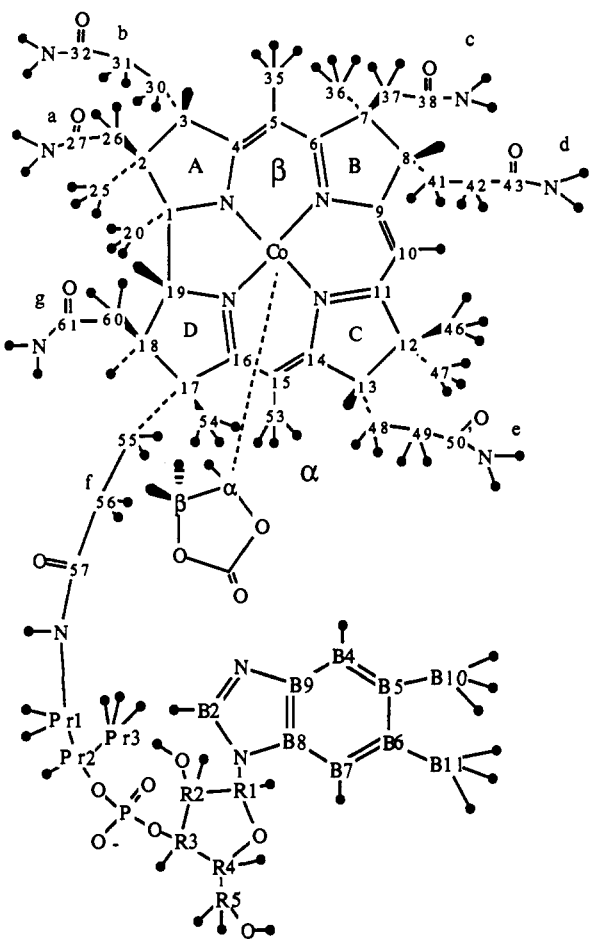

Figure 4. Alphabetical and numerical labeling scheme for the 2-D NMR discussion. Note that the exact conformation found for α_1-**1** by 2-D NMR is somewhat different than illustrated by this schematic drawing. For example, the benzimidazole base is found to be upside down relative to what is shown, and the absolute configuration at the chiral carbon (C_α) attached to Co is not known with certainty.

visible spectra are identical]. In the case of **2**, both base-on and protonated base-off visible spectra can be observed. (As expected, the protonation of the benzimidazole base in **1** does cause the expected increase in the UV absorbance from 275 to 290 nm assigned to the benzimidazole.[20]) These results for the alkylcobalamin **1** are possible only when the alkyl group occupies and thus blocks cobalt's α coordination site; (7) the finding that **1** can be converted to a β-base-on form with a UV–visible spectrum very close to α-base-on **2** (Figure D, supplementary material) by the addition of exogenous 1-methylimidazole or pyridine,[21] proving that a binding site on cobalt is still available—the β-axial position is the only such site in **1**; and finally (8) the finding that photolytic cleavage of the Co–C bond in **1** leads primarily to **2**, again demonstrating that **1** and **2** are isomers (differing only in the α vs β position of their Co–C bond).

Initial evidence that **1** exists as a mixture of two diastereomers came from the 1-D ^{1}H NMR. The ^{1}H NMR spectrum of **1** in acidic (0.7 M DCl) D_2O, Figure 3, is similar to that of a typical base-off β-alkylcobalamin, for example, **2**. The chemical shift for the protonation-sensitive benzimidazole B2 proton of **1** at 9.1 ppm indicates a fully protonated benzimidazole nitrogen (pK_a = 5.3 ± 0.3, measured by a NMR titration);[22] see Figure 4 for the

(18) Three matrices were used for FAB-MS spectroscopy with different results: *m*-nitrobenzyl alcohol produced the best results, nitrophenyl octyl ether gave a much weaker molecular ion peak, and a (1:5) dithioerythritol/dithiothreitol matrix gave an even weaker molecular ion peak.

(19) (a) Finke, R. G.; McKenna, W. P.; Schiraldi, D. A.; Smith, B. L.; Pierpont, C. *J. Am. Chem. Soc.* **1983**, *105*, 7592. (b) Finke, R. G.; Schiraldi, D. A. *J. Am. Chem. Soc.* **1983**, *105*, 7605.

(20) Hill, J. A.; Pratt, J. M.; Williams, R. J. P. *J. Theor. Biol.* **1962**, *3*, 423.

(21) Upon addition of nitrogenous bases, such as 1-methylimidazole or pyridine, a spectrum very similar to the base-on cobalamin **2** is obtained, Figure D (supplementary material). The two peaks for **1** at 337 and 368 nm have identical peak locations but different peak intensities compared to **2**; the peak for **1** at ca. 523 nm has shifted 4 nm to 527 nm in **2**, but has a very similar peak shape.

Table I. ^{1}H NMR Chemical Shift and Signal Assignments for the Nucleotide Loop and Select Corrin Protons of α-(2-Oxo-1,3-dioxolan-4-yl)cobalamin and Comparisons to the Corresponding Signals in α-Ribazole 3′-Phosphate at pH 8.6 and pH 3.0, (5′-Deoxyadenosyl)cobalamin (Coenzyme B_{12}) at pH 2.1 and pH 7.0, and Cyanocobalamin[a]

assignment	α-Cbl[b]	α-ribazole phosphate[c]	α-ribazole phosphateH$^+$[c]	coenzyme (base-off)[d]	coenzyme (base-on)[e]	CNCbl[f]
B2	8.35	8.41	9.13	9.16	6.95	7.08
B4	7.37	7.46	7.41	7.44	6.24	6.50
B7	7.31	7.35	7.18	7.55	7.16	7.27
R1	6.30	6.38	6.41	6.56	6.26	6.35
R2	4.84	4.71	4.96	4.97	4.23	4.27
R3	4.84	4.71	4.84	4.83	4.72	4.70
R4	4.44	4.52	4.60	4.79	4.10	4.06
R5	3.79	3.95, 3.88	3.95, 3.85	3.94, 3.84	3.88, 3.74	3.92, 3.74
Pr1	3.55, 3.18			3.38, 3.27	3.54, 3.16	3.60, 2.95
Pr2	4.38			4.36	4.33	4.34
Pr3	1.32			1.23	1.21	1.25
C10	6.44			6.97	5.93	6.08
C20	1.16			0.81	0.47	0.45

[a] Shifts relative to internal trimethylsilyl propionate, except α-ribazole phosphate shifts relative to DSS. [b] This work. [c] Reference 32. [d] Reference 28. [e] Reference 27. [f] Reference 33.

labeling scheme used for the H and C atoms in **1**.[23] However, for **1** *all the benzimidazole protons (the downfield region) are apparent doublets* (Figure 3), as expected when two α-type diastereomers are present since the benzimidazole and its protons are close in space to the chiral carbon bonded to cobalt. This is unlike **2**, whose protonated benzimidazole exhibits a ^{1}H NMR spectrum showing B2, B4, and B7 hydrogens as *singlets* and only the C10 proton on the corrin as an apparent doublet (actually two peaks for two different diastereomers), because now only the C10 proton is near the chiral carbon in diastereomeric **2**. (These 1-D NMR data by themselves establish that the ethylene carbonate alkyl group must be close to the benzimidazole in **1**.) In neutral D_2O the B2 hydrogen of the benzimidazole base in **1** is shifted 0.9 ppm upfield[22] but still exhibits two peaks, possibly indicating the presence of a so-called "tuck-in" form of the axial base,[24] although no evidence for this is found in the 2-D NMR studies of the α_1 diastereomer of **1** (vide infra).

Separation of 1 into Its Two Diastereomers. HPLC studies showed that **1** could be separated into two peaks in an approximately 55:45 mol % ratio of diastereomers by changing the HPLC conditions from 25% NH_4OAc/75% CH_3CN, on an analytical reversed-phase C-18 column, to 86% H_2O/14% CH_3CN, now using a semipreparative reversed-phase C-18 column. Pure samples of the two (α_1-**1** and α_2-**1**) diastereomers could be obtained in milligram quantities by collecting the HPLC effluent and removing the solvent by first rotary evaporation and then freeze-drying. By this means it was possible, albeit time consuming (requiring ~1 h/mg), to obtain enough of the first diastereomer off the column (α_1-**1**) in greater than 97% purity (by HPLC and 1-D NMR) in order to perform various experiments including 2-D NMR and determination of its 5,6-dimethylbenzimidazole base pK_a. The second, α_2-**1**, diastereomer could occasionally be obtained in >95% pure form (by HPLC), but it is less stable (both thermally and photochemically, vide infra) than the α_1-**1** diastereomer, and thus we did not attempt to study its physical properties.

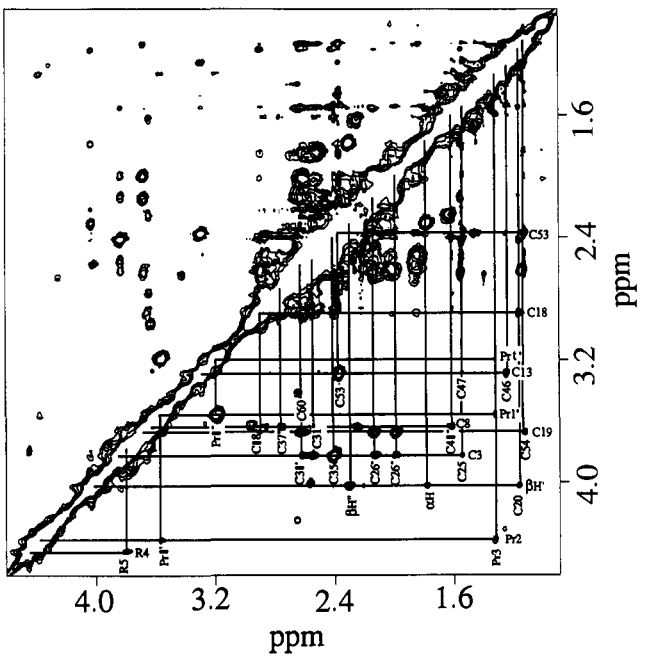

Figure 5. Part of the phase-sensitive 2-D NOE spectrum of α_1-**1**. Lines drawn indicate the NOE connectivities of the molecule.

2-D NMR Spectroscopy of the α_1-1 Diastereomer. The labeling and proton and carbon numbering scheme that will be used throughout the 2-D NMR presentation is shown in Figure 4. Most of the ^{1}H NMR spectrum of the α_1 diastereomer, α_1-**1**, was assigned from NOESY[25] and HOHAHA (homonuclear Hartmann–Hahn)[26] spectra by using strategies described previously.[27-29]

(22) (a) As detailed in the Experimental Section and shown in Figure J (supplementary material), a preliminary value for the pK_a of the benzimidazole in α_1-**1** and α_2-**1** of 5.4 ± 0.3 was obtained by following the chemical shift of the benzimidazole B2 hydrogen as a function of the solution pH [pH(apparent), in D_2O, 22 °C, at ionic strength I = 0; see the Experimental Section for the controls and other data[56] that allow the conversion of these measurements in D_2O to pK_a values in H_2O]. Such pK_a measurements for α-cobalamins are of a more fundamental interest, since only two (not three) equilibrium constants (so-labeled "K_{Bz} and K_H") plus any possible tuck-in form[22b,c,24] are all that are involved in the somewhat simplified α-alkyl systems. Hence, the measurement and then comparison (under carefully chosen, identical conditions) of accurate α-alkylcobalamin apparent pK_a values to literature K_{obs} and literature K_{Bz} and K_H values[22b,c] should provide additional information on the nature of the base-on/base-off equilibria and conformations in alkylcobalamins. Note that the easily measured α_1-**1** and α_2-**1** pK_a values reported herein of pK_a = 5.4 ± 0.3 yielded, as they should have, values close to the more precisely measured[22b,c] pK_a for the simple base α-ribazole [pK_a = 5.56 (H_2O, 25 °C, I = 1.0 M)]. (b) Brown, K. L. *J. Am. Chem. Soc.* **1987**, *109*, 2277–2284. (c) Brown, K. L.; Peck-Siler, S. *Inorg. Chem.* **1988**, *27*, 3548–3555.

(23) Brodie, J. D.; Poe, M. *Biochemistry* **1972**, *11*, 2534–2542.

(24) The recently characterized tuck-in form of certain alkylcobalamins involves the unprotonated benzimidazole in a conformation "tucked under" the corrin ring, eq 1. In the case of methylcobalamin, careful ^{13}C NMR studies suggest that the B3 hydrogen of the benzimidazole is hydrogen bonded to the e side chain of the cobalt corrin in the tuck-in form.[22b,c]

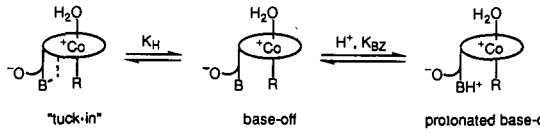

(1)

(25) Jeener, J.; Meier, B. H.; Bachmann, P.; Ernst, R. R. *J. Chem. Phys.* **1979**, *71*, 4546–4553. Kumar, A.; Ernst, R. R.; Wüthrich, K. *Biochem. Biophys. Res. Commun.* **1980**, *95*, 1–6.

(26) Braunschweiler, L.; Ernst, R. R. *J. Magn. Reson.* **1983**, *53*, 521–528. Davis, D. G.; Bax, A. *J. Am. Chem. Soc.* **1985**, *107*, 2820–2821. Bax, A.; Davis, D. G. *J. Magn. Reson.* **1985**, *65*, 355–360.

(27) Summers, M. F.; Marzilli, L. G.; Bax, A. *J. Am. Chem. Soc.* **1986**, *108*, 4285–4294.

Table II. ^{13}C NMR Chemical Shift and Signal Assignments for the Nucleotide Loop and Select Corrin Carbons of α-(2-Oxo-1,3-dioxolan-4-yl)cobalamin and Comparisons to the Corresponding Signals in α-Ribazole 3′-Phosphate at pH 8.36 and pH 2.94, Dicyanocobalamin, (5′-Deoxyadenosyl)cobalamin (Coenzyme B_{12}) at pH 2.1 and pH 7.0, and Cyanocobalamin[a]

assignment	α-Cbl[b]	α-ribazole phosphate[c]	α-ribazole phosphateH^+[c]	coenzyme (base-off)[d]	$(CN)_2$Cbl[e]	coenzyme (base-on)[e]	CNCbl[f]
B2	145.3	145.5	140.8	141.4	145.1	144.7	144.7
B4	121.2	121.1	116.5	117.2	121.6	121.4	119.3
B5	134.8	134.1	139.7	139.6	135.0	134.5	135.8
B6	135.9	135.0	139.6	139.6	135.8	136.8	137.9
B7	113.0	113.6	115.0	115.7	113.6	113.5	114.3
B8	134.5	136.0	131.2	132.1	134.1	133.3	132.8
B9	142.5	142.7	131.4	132.6	142.9	141.0	139.5
B10	22.4	22.2	22.3	22.6	22.7	22.5	22.8
B11	22.4	21.9	22.1	22.7	22.2	22.3	22.2
R1	87.7	88.4	89.6	90.2	88.3	89.4	89.8
R2	74.1	74.1	74.1	74.5	73.7	72.0	71.7
R3	77.2	75.7	76.7	77.6	76.7	76.2	75.9
R4	87.2	86.0	88.2	89.2	85.6	84.6	84.9
R5	64.1	64.0	63.8	64.1	63.5	63.4	63.3
Pr1	47.7			48.9	47.5	47.8	48.3
Pr2	75.3			75.2	74.9	76.0	75.8
Pr3	21.9			21.5	21.3	21.7	21.9
C10	97.3			100.4	93.7	97.7	97.7
C20	25.2			26.7	21.7	23.5	22.1
C49	34.8			35.0	35.6	38.1	37.5

[a] Shifts relative to internal trimethylsilyl propionate. [b] This work. [c] Reference 22b. [d] Reference 28. [e] Reference 27. [f] Reference 34.

Since it is sometimes extremely difficult to distinguish between direct and relayed connectivities in the HOHAHA experiment,[27] an experiment with a short mixing time (10.6 ms) was used to determine the direct connectivities that were undistinguishable from the relayed connectivities in the HOHAHA experiment with a longer mixing time (105.9 ms), Figure E (supplementary material). The ethylene carbonate signals were identified by their connectivity pattern in the HOHAHA spectra. A peak at 4.0 ppm in the ^1H NMR spectrum shows connectivities to peaks at 2.32 and 1.80 ppm in both HOHAHA spectra, indicating that three protons are directly coupled to each other. No relayed connectivities are seen for these three protons. Nowhere else in the molecule are there three protons that are directly coupled to each other and that would show no relayed connectivities. The peak at 4.0 ppm shows an NOE in the NOESY spectrum, Figure 5, to C20 H_3 and a weak NOE to B7 H. Since C20 H_3 is known to point down from the α face and the benzimidazole moiety (containing B7 H) is known to be appended to the α face, this NOE pattern is very strong evidence that α_1-**1** is an α-alkylcobalamin.

Most of the ^{13}C NMR spectrum of α_1-**1** was assigned from HMQC (^1H-detected heteronuclear multiple quantum coherence)[30] spectra, Figure F (supplementary material) and Figure 6, and HMBC (heteronuclear multiple bond correlation)[31] spectra, Figure G (supplementary material), using strategies described previously.[27-29] The ^1H and ^{13}C NMR shifts of the nucleotide loop of α_1-**1** give further evidence that the alkyl group is attached to Co on the α face instead of the benzimidazole moiety. As can be seen in Table I,[32] the ^1H NMR shifts of B2 H, B4 H, and B7 H are quite similar to those of α-ribazole phosphate. These protons, and others,[33] have quite different shifts if one compares

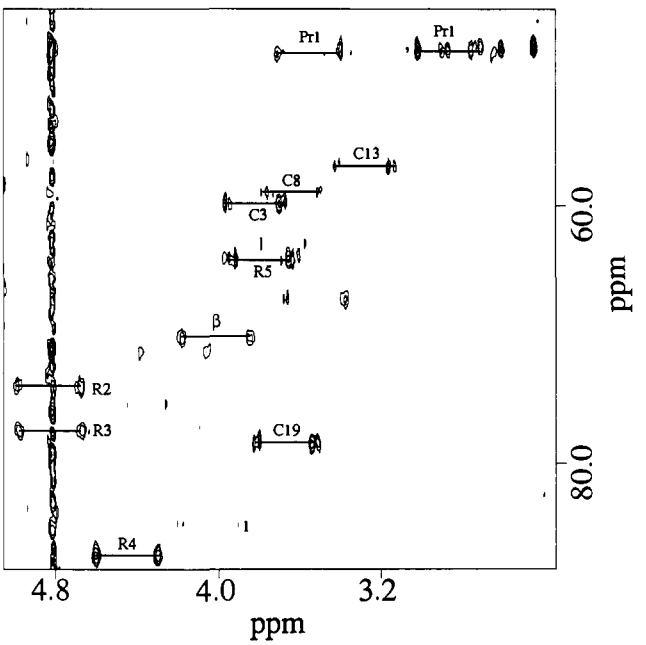

Figure 6. Part of the HMQC spectrum of α_1-**1** showing the methine proton region. The center of each pair of cross peaks connected with a drawn line corresponds to the proton chemical shift. The cross peaks in a given pair are separated by a distance equal to the ^1H–^{13}C coupling constant.

base-on cobalamins to either α-ribazole phosphate or base-off cobalamins.

As can be seen in Table II,[34a] the ^{13}C NMR shifts of the nucleotide loop also provide evidence that α_1-**1** is an α-alkylcobalamin. The ^{13}C NMR shifts of R2 and R4 are more similar to α-ribazole phosphate and the base-off cobalamins [dicyano-

(28) Bax, A.; Marzilli, L. G.; Summers, M. F. *J. Am. Chem. Soc.* **1987**, *109*, 566–574.

(29) Pagano, T. G.; Yohannes, P. G.; Hay, B. P.; Scott, J. R.; Finke, R. G.; Marzilli, L. G. *J. Am. Chem. Soc.* **1989**, *111*, 1484–1491.

(30) Müller, L. *J. Am. Chem. Soc.* **1979**, *101*, 4481–4484. Bax, A.; Subramanian, S. *J. Magn. Reson.* **1986**, *67*, 565–569.

(31) Bax, A.; Summers, M. F. *J. Am. Chem. Soc.* **1986**, *108*, 2093–2094.

(32) (a) References in Table I: Brown, K. L.; Hakimi, J. M. *J. Am. Chem. Soc.* **1986**, *108*, 496–503. (b) Hensens, O. D.; Hill, H. A. O.; McClelland, C. E.; Williams, R. J. P. In B_{12}; Dolphin, D., Ed.; Wiley-Interscience: New York, 1982; Vol. 1, Chapter 13, and references therein.

(33) The shift of B4 H is similar to base-off coenzyme B_{12} and quite different from the base-on form. The shift of B4 H in base-on cobalamins is significantly upfield to its shift in α-ribazole phosphate and base-off cobalamins, most likely due to the corrin ring anisotropy. The shift of B2 H in α_1-**1** is quite different from its shift in N3-benzimidazole protonated base-off coenzyme B_{12}. Also, the shift of C20 H_3 in α_1-**1** is more similar to base-off coenzyme B_{12} than to base-on cobalamins.

(34) (a) Reference in Table II: Pagano, T. G.; Marzilli, L. G. *Biochemistry* **1989**, *28*, 7213–7223, and references therein. (b) Additional evidence can be found from the shift of C49 of the *e*-propionamide side chain. Its shift in α_1-**1** is very similar to $(CN)_2$Cbl and base-off coenzyme B_{12}, but significantly different from the base-on cobalamins. The *e*-propionamide side chain is known to be hanging from the α face and the upfield shift of this carbon in the base-off cobalamins is thought to be due to a repositioning of the side chain due to a loss of steric interactions with the benzimidazole moiety.[28] All of the ^{13}C NMR shifts discussed above are at least 0.5 ppm different from those of base-on cobalamins. These shifts suggest that the benzimidazole moiety is not attached to Co, but instead is hanging free in α_1-**1** as it is in $(CN)_2$Cbl and base-off coenzyme B_{12}.

cobalamin ($(CN)_2$Cbl) and base-off coenzyme B_{12}] than the base-on cobalamins [cyanocobalamin (CNCbl) and base-on coenzyme B_{12}]. For example, the shifts of R1, B6, and B9 are similar in α_1-**1**, α-ribazole phosphate, and $(CN)_2$Cbl. The shifts of R3 and Pr2 are similar in α_1-**1**, base-off coenzyme B_{12}, and $(CN)_2$Cbl. The shift of R5 is similar in α_1-**1**, α-ribazole phosphate, and base-off coenzyme B_{12}.[34b]

An indication of the position of the benzimidazole moiety in α_1-**1** is given from the NOESY spectrum and certain ^{13}C NMR shifts. In addition to the NOE between one of the ethylene carbonate signals and C20 H_3 mentioned above, there is also a weak NOE between B7 H and C20 H33. These NOEs indicate that the benzimidazole moiety in α_1-**1** is repositioned upside down as it is in base-off coenzyme B_{12}.[28] There is no evidence for hydrogen bonding between B3 and an e side chain amide hydrogen as is observed for $(CN)_2$Cbl.[22b] (C49 is shifted downfield in $(CN)_2$Cbl due to the hydrogen bonding of the e side chain to B3.) The shift of C49 in α_1-**1** (34.8 ppm) is closer to that of base-off coenzyme B_{12} (35.0 ppm) and dicyanocobinamide[22b] (35.1 ppm), where the dimethylbenzimidazole nucleotide is absent, than to $(CN)_2$Cbl (35.6 ppm). In an upside-down benzimidazole, B3 cannot hydrogen bond to the e side chain.

From ^1H and ^{13}C chemical shifts of the alkyl group, in conjunction with the NOESY spectrum, the orientation and an approximate location of the alkyl group can be determined; however, an assignment of the absolute stereochemistry of the α_1-**1** diastereomer has not proven possible. As discussed above, the three proton signals of the alkyl group were found at 4.0, 2.32, and 1.80 ppm. We identify these protons as α-H for the proton on the α-carbon bound to cobalt and β-H′ and β-H″ for the downfield and upfield signals, respectively, of the protons attached to the carbon β to the cobalt. From the HMQC spectrum, Figure F (supplementary material) and Figure 6, we found that the carbon to which the proton giving rise to the signal at 4.0 ppm is attached has a shift of 70.1 ppm. From ^{13}C NMR studies of a model compound[19] (2-oxo-1,3-dioxolan-4-yl)Co[C_2(DO)$(DOH)_{pn}$]Cl, where [C_2(DO)$(DOH)_{pn}$] = 2,10-diethyl-3,9-dimethyl-1,4,8,11-tetraazaundeca-1,3,8,10-tetraene-1,1-diol, we found, using an ATP (attached proton test)[35] experiment, that the carbon of the alkyl group containing two protons has a shift of 70.4 ppm. Therefore, the ^1H signal at 4.0 ppm in α_2-**1** is due to the proton attached to the carbon β to the cobalt, that is, the one containing two protons. It was not possible to obtain information on the carbons of the 2.32 and 1.80 ppm signals from the HMQC spectrum of α_2-**1**. In the model compound it was found[19] that the two protons on the β-carbon gave rise to signals at 4.07 and 4.13 ppm and the α-H gave rise to a signal at 3.67 ppm. Two of the three signals for the alkyl group in **1** (those at 2.32 and 1.80 ppm) are shifted dramatically upfield from their shifts in the model compound.[36a]

Signals for protons closer to the corrin ring and Co in α_2-**1** should be shifted upfield relative to the model compound. The α-carbon is tetrahedral and the plane of the ring of the alkyl group must lie at an angle to the plane of the corrin ring. Also, the bond connecting the two protonated carbons of the alkyl group is expected to be tilted away from the plane of the corrin ring. This orientation of the alkyl group places the α-proton in the same position relative to Co as the Co–CH_3 group in MeCbl. The more electron rich corrin system should lead to an upfield shift of this proton relative to its shift in the model compound.[36a] Therefore, the signal at 1.80 ppm is assigned to this proton. Of the other two protons, β-H″ is closer to Co and the corrin ring due to the tilt of the plane of the ring of the alkyl group. This proton most likely gives rise to the signal at 2.32 ppm. β-H′ is the farthest from the corrin ring and its signal is expected to be shifted only slightly upfield from where it is found in the model compound. The signal at 4.0 ppm is assigned to this proton.

These assignments agree with the conclusions based on the HMQC and APT experiments that the 4.0 ppm signal is for a proton on the β-carbon. The NOESY spectrum adds further confirmation to these assignments. The signal at 1.80 ppm shows no cross peaks except to the 2.32 and 4.0 ppm signals. These two signals show NOEs to C20 H_3 in the NOESY spectrum. The signal at 2.32 ppm shows a much weaker NOE to C20 H_3 than the signal at 4.0 ppm. C20 H_3 is the only corrin proton signal that shows an NOE to either of these two protons. The lack of NOEs from the alkyl group protons to C25 H_3 or C18 H suggests that the alkyl group lies along a line from the cobalt to C1 or alternatively between C1 and C19. β-H′ is closer to C20 H_3 than β-H″, based on the relative intensities of their NOEs. Finally, the B7 H signal has NOE cross peaks to both C20 H_3 and β-H′. These NOE cross peaks suggest that the nucleotide loop is in a conformation similar to that found in protonated base-off coenzyme B_{12}[28] instead of the tuck-in conformation[22b,c,24] found for nonprotonated base-off cobalamins. Furthermore, the B7 H–β-H′ cross peak confirms that the 4.0 ppm signal is due to β-H′, which is pointed away from the corrin.

Overall, the 2-D NMR studies provide additional unequivocal evidence that α_1-**1** is an α-alkylcobalamin. They do not, however, allow us to assign the absolute stereochemistry of this diastereomer.

Further Studies of the Physical Properties of 1. The studies provided below are of interest since almost no reliable information exists in the literature comparing the physical properties of α- vs β-alkylcobalamins (see ref 8c, however), and certainly no data at all comparing two α diastereomers. The following studies, other than the thermolyses and photochemical stability controls, were performed prior to our development of the α_1-**1** from α_2-**1** separation methodology, and thus on **1** as a roughly equimolar mixture of its α_1 and α_2 diastereomers. Hence, except where noted otherwise, the following results (or numerical values) are composites of the individual results for α_1-**1** plus α_2-**1** diastereomers. The time and expense of future work examining the individual diastereomers may be justified in selected cases, for example, where a specific physical property or a quantitatively reliable measurement is of special interest.

Differential Thermal Stability of the α_1-1 and α_2-1 Diastereomers. Because the separated diastereomers appeared to have different stabilities, half-lives for the aerobic thermal decomposition of each diastereomer were measured in H_2O (solution pH 5.8). The half-lives for the α_1-**1** and α_2-**1** diastereomers at 40 and 54 °C are as follows: α_1-**1**, 250 ± 16 (40 °C) and 41 ± 5 h (54 °C); α_2-**1**, 93 ± 10 (40 °C) and 10 ± 2 h (54 °C). In other words, the α_1-**1** diastereomer is ca. 2.7–4.1 times as stable as the α_2-**1** diastereomer, depending on the temperature.

Approximate half-lives for photolysis under low light conditions (an AA flashlight in an otherwise dark room) were also measured, experiments designed to approximately simulate those plausibly encountered in a darkroom where, for example, chromatography was performed. The results *document the extreme light sensitivity of α_1-1 and α_2-1 even to an AA flashlight*, half-lives of 90 ± 10 and 60 ± 10 s, respectively, under the dilute, ca. 1×10^{-4} M, and other exact conditions given in the Experimental Section (see Handling of Light-Sensitive Materials). It is almost surely this extreme light sensitivity that accounts for (1) the apparent "erratic stability" of α_1-**1** and α_2-**1** noticed in our early work in this area and (2) the fact that special care and nearly light-free handling were required to get the 2-D NMR spectra of α_1-**1** reported herein (i.e., without the ca. 30% decomposition to Co^{III}-B_{12a} observed in our early attempts).

Axial Base Equilibrium Constant. The equilibrium constant for nitrogenous base coordination to the β-axial position in the diastereomeric α-alkylcobalamin, **1**, was determined since such binding constants are not available currently for any α-alkylcobalamin. The K_{eq} data are collected in Table III (including the literature cobinamide data cited);[37,38] the equilibrium constants

(35) Patt, S. L.; Shoolery, J. N. *J. Magn. Reson.* **1982**, *46*, 535–539.
(36) (a) In general, ^1H NMR shifts in these types of complexes can be influenced by: (i) inductive effects, (ii) anisotropy of the equatorial ligand, and (iii) anisotropy of the Co.[36b] (Further discussion of these factors is provided as supplementary material). (b) Parker, W. O., Jr.; Zangrando, E.; Bresciani-Pahor, N.; Randaccio, L.; Marzilli, L. G. *Inorg. Chem.* **1986**, *25*, 3489–3497. (c) Parker, W. O., Jr.; Zangrando, E.; Bresciani-Pahor, N.; Marzilli, P. A.; Randaccio, L.; Marzilli, L. G. *Inorg. Chem.* **1988**, *27*, 2170–2180.

(37) Pailes, W. H.; Hogenkamp, H. P. C. *Biochemistry* **1968**, *7*, 4160.

Table III. K_{eq} Values for Axial Base Binding Co(α-R) + Base $\rightleftarrows$ (β-Base)Co(α-R) in Comparison to Literature (β-R)Co + Base $\rightleftarrows$ (β-R)Co(α-Base) Axial Base K_{eq} Values

compound	conditions	added base	log K_{eq}	ref
Co(α-R)cobalamin **1**	H_2O,[a] 22 °C	1-methylimidazole	1.95 (1)	*c*
		pyridine	1.37 (2)	*c*
		(±)-histidine	1.1 (1)	*c*
		1,5,6-trimethylbenzimidazole	0.6 (1)	*c*
(β-R)Co-cobinamides				
methyl	H_2O	pyridine[b]	1.04	37
methyl	pH 8.8, 25 °C	imidazole[b]	0.9	38
ethyl	pH 8.8, 25 °C	imidazole[b]	−0.5	38
isopropyl	pH 8.8, 25 °C	imidazole[b]	<−1.9	38
neopentyl	pH 8.8, 25 °C	imidazole[b]	−1.4	38
cyclohexyl	pH 8.8, 25 °C	imidazole[b]	−1.9	38

[a] pH_{init} = ~6. [b] Error estimates are not available for these literature data. [c] Present work.

Scheme III

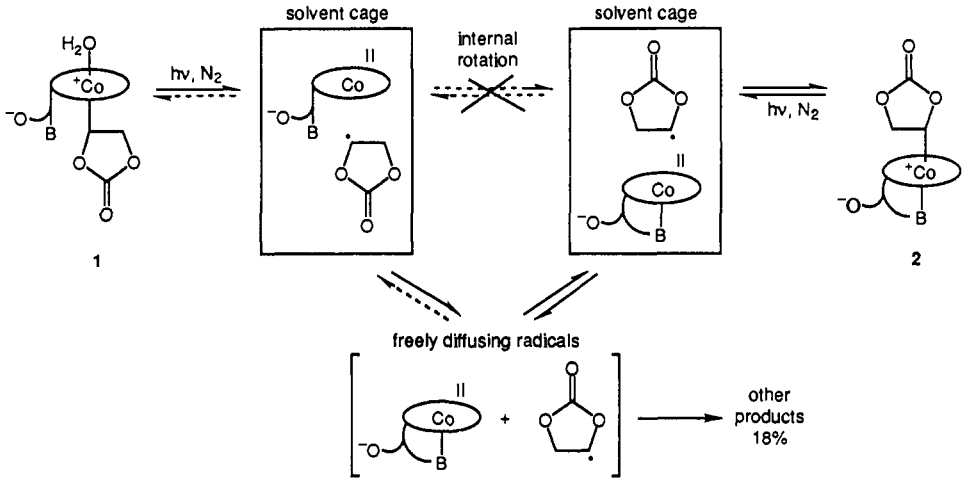

follow the trend 1-methylimidazole > pyridine > histidine > 1,5,6-trimethylbenzimidazole. The trend is consistent with the steric demand of the axial base; increasing the axial base size decreases the binding constant. Note that the K_{eq} for 1-methylimidazole binding is the highest measured K_{eq} value for 5-coordinate alkylcobinamides studied to date (see Table III). This can be rationalized by the strong electron-withdrawing ability of the ethylene carbonate alkyl group, as it is well established in alkylcobalamins that electron-withdrawing alkyl groups favor stronger binding of electron-donating axial bases.[39] (The β face is also thought to be sterically less congested compared to the α face of a cobalamin.[12]) Another apparent effect of the electron-withdrawing alkyl group in **1** is the finding that pyridine binds significantly less well than 1-methylimidazole. Unfortunately, reliable data with error bars for β-alkylcobalamins, under identical pH conditions, are not available for comparative purposes.

Conversion of α-1 to β-2 by Anaerobic Photolysis. Note that the conversion of α-**1** to β-**2** should be exothermic and probably exergonic since the appended 5,6-dimethylbenzimidazole axial base can coordinate to cobalt in the β-alkyl, β-**2** (K_{eq} > 1 at 25 °C). This suggested to us that photolysis of the (therefore) kinetic product, *base-off* α-**1**, should yield at least some of the thermodynamic product, *base-on* β-**2**. This follows since the expected sequence of reactions is as follows: Co–C photohomolysis to produce the intermediates Co^{II}-B_{12r} and the 1,3-dioxolan-4-yl radical, followed by recombination of the 1,3-dioxolan-4-yl radical with *base-on*[15] Co^{II}-B_{12r}, which should form **2** but not **1** (except perhaps by in-cage recombination),[40a,b] since the benzimidazole axial base blocks the α face by its coordination to cobalt.

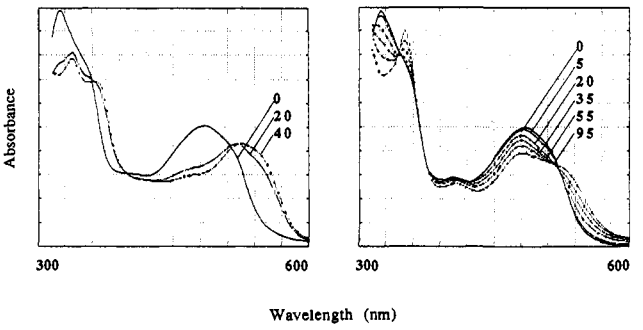

Figure 7. Overlayed spectra for the anaerobic photolysis of **1**. Left: in deionized H_2O; Right: in the presence of 220 equiv of TEMPO. The photolysis time (seconds) prior to each spectrum is labeled in the figure.

Anaerobic photolysis of **1** in deionized H_2O does indeed convert **1** to >80% **2** (exposure of the solution to air and then HPLC analysis after 70 s of photolysis gave 82% of **2** and 18% of Co^{III}-B_{12a} with no detectable **1**). The conversion is irreversible, further anaerobic photolysis of the product **2** producing Co^{II}-Br_{12r} (Figure 7), an independently established photolysis product of **2**.[17]

One can ask whether or not the conversion of **1** to **2** involves caged-radical pairs[40a,b] or freely diffusing Co^{II}-B_{12r} and alkyl radicals. This question was examined by photolysis of **1** in the presence of 200 equiv (ca. 10^{-2} M) of the radical-trapping reagent, TEMPO (2,2,6,6-tetramethylpiperidinyl-1-oxy). At such (lower) concentrations of TEMPO, only the trapping of free (as opposed to caged) radicals is known to occur, at least for systems like

(38) Baldwin, D. A.; Betterton, E. A.; Chemaly, S.; Pratt, J. M. *J. Chem. Soc., Dalton Trans.* **1985**, 1613.

(39) Hogenkamp, H. P. C.; Rush, J. E.; Swenson, C. A. *J. Biol. Chem.* **1965**, *240*, 3641. X-ray crystallography also reveals such an electronic effect. For example, the axial benzimidazole Co–N (1.97 Å) bond distance is short for cyanocobalamin with its electron-withdrawing CN group, while it is relatively long (Co–N 2.19 Å) for methylcobalamin with its electron-donating methyl group: Rossi, M.; Glusker, J. P.; Randaccio, L.; Summers, M. F.; Toscano, P. J.; Marzilli, L. G. *J. Am. Chem. Soc.* **1985**, *107*, 1729.

(40) (a) Koenig, T.; Finke, R. G. *J. Am. Chem. Soc.* **1988**, *110*, 2657. (b) Koenig, T. K.; Hay, B. P.; Finke, R. G. *Polyhedron* **1988**, *7*, 1499–1516. (c) Finke, R. G.; Garr, C., unpublished results (demonstrating the conditions required to trap caged-radical pairs).

Scheme IV

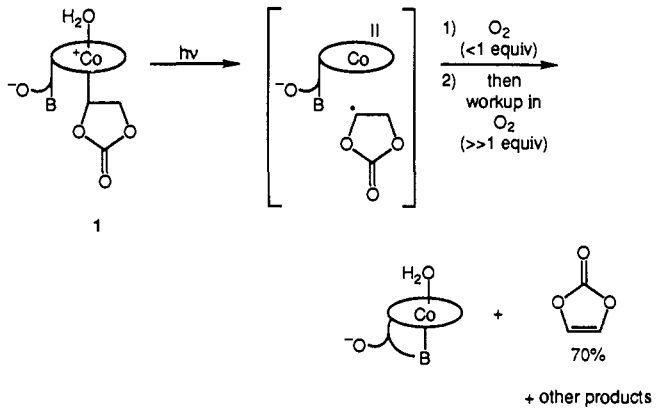

adenosylcobalamin (coenzyme B_{12}).[40c] In the presence of 10^{-2} M TEMPO, 5 s of photolysis of α-**1** produces mostly Co^{II}-B_{12r} but, as expected, no β-**2** (Figure 7) (with perhaps some remaining **1**, since the spectrum of Co^{II}-B_{12r} and **1** are very similar). The clean isosbestic points indicate that the conversion of α-**1** to Co^{II}-B_{12r} is finished within ~20 s of photolysis; after this the spectrum shows a mixture of Co^{II}-B_{12r} and Co^{III}-B_{12a} (the latter from the established[41] redox reaction *in* H_2O of Co^{II}-B_{12r} with TEMPO to produce Co^{III}-B_{12a} and $TEMPO^-H^+$).

Although photolysis of **1** should produce initially an α-structure caged-radical pair (i.e., Co^{II}-B_{12r} and 1,3-dioxolan-4-yl radicals with an α orientation), the fact that the formation of **2** can be *totally* inhibited by even 10^{-2} M TEMPO indicates that the conversion of **1** to **2** involves *only* free- and not caged-radical processes,[40a,b] Scheme III. Restated, the internal rotations of the large Co^{II}-B_{12r} and 1,3-dioxolan-4-yl radical relative to one another (thereby interconverting an α- to a β-radical pair) are noncompetitive relative to their faster, diffusive cage escape in weaker solvent cages[40a,b] like 25 °C H_2O. Diffusional reencounter with *α-base-on*[15b] Co^{II}-B_{12r} can produce only the new, β-structure radical pair, which then collapses to β-**2**.

Generally consistent with the above findings is the fact that photolysis in H_2O converts α-methylcobalamin to 93% β-methylcobalamin (plus 7% α-methylcobalamin);[9] it would be of interest to see if added TEMPO can completely inhibit this α to β conversion reaction. Furthermore, in α-methyl-β-cresoyl*cobamide*, photolysis yields an equilibrium mixture that is essentially statistical, 50% α- and 50% β-methylcobamide isomers.[9] (Cobamides are B_{12}-type corrin complexes where the appended β-5,6-dimethylbenzimidazole axial base has been removed and replaced, in the present case probably by H_2O, since the cresoyl (phenyl) group cannot serve as an axial base.)

Aerobic Photolysis of 1. The aerobic photolysis of **1** in pH 7 phosphate buffer proceeded with clean isosbestic points to produce Co^{III}-B_{12a} (characteristic λ_{max} at 351 nm) and, interestingly, 70 ± 10% vinylene carbonate, Scheme IV (^1H NMR, 7.4 ppm; IR, two characteristic peaks at 1803 and 1835 cm^{-1}). These results are unexceptional except for the high yield of *the olefin* vinylene carbonate (which has some precedent[42] in the increased yields of ethylene and propene seen in the aerobic photolysis of ethylcobalamin and isopropylcobalamin[17b]). Given the TEMPO-trapping results in the previous section (which show the formation of freely diffusing radicals), the radical-cage formation of vinylene carbonate and hydridocobalamin (H–Co) cannot be occurring. Furthermore, O_2 capture of free radicals is typically diffusion controlled, but the resultant $RO_2^{\bullet}$ radical invariably gives products containing a R–O bond but no olefins. Hence, the unexplained mechanism operating here is of some interest.

The key appears to be the conditions of the experiment where less than 1 equiv of O_2 (2.5×10^{-4} M O_2)[42c] is present in the unstirred, closed reaction vessels (see the Experimental Section for further details). If Co^{II}-B_{12r} were to selectively capture (substoichiometric) O_2 under these conditions [especially in the NMR and IR experiments, which employed higher, $(1-7) \times 10^{-3}$ M, concentrations of **1**], then the resultant B_{12}-Co–O–O$^{\bullet}$ could conceivably abstract a H$^{\bullet}$ from the 2-oxo-1,3-dioxolan-4-yl radical to give vinylene carbonate and, initially, B_{12}-Co–O–O–H. Obviously, any future studies of this reaction should pursue product studies (organic and O_2 products) as a function of the solution O_2 concentration.[42]

Deprotection of 1 in pH 10. Our earlier and extensive studies of **2**, originally prepared to probe the so-called "cobalt participation or nonparticipation question",[17,19] have confirmed that the carbonate group in **2** (and thus probably also in **1**) is subject to base deprotection (removal) as CO_3^{2-}. Moreover, the relative reactivity of **1** and **2** to base deprotection in aerobic pH 10 borate aqueous buffer is of some interest as a measure of the steric crowding of the α and β faces of **1** compared to **2**.

The results are that **1** is slightly more stable, $t_{1/2}$ for **1** is 230 min at 22 °C at pH 10, in comparison to **2**, $t_{1/2}$ is 155 min at 22 °C and pH 10. They suggest that the β face in **2** is slightly less shielded than the α face in **1**, although we caution against overinterpretation of these half-lives, each of which is a composite of the individual reactivity of two diastereomers toward base.

Discussion

Perhaps the most interesting unanswered question is what the mechanisms are leading to α- vs β-alkylcobalamins and other cobamides, and what factors control the α vs β ratio. Although the literature indicates that the lower (α) side of the cobalt corrin in B_{12} is believed to be sterically more "crowded" than the upper (β) side,[12] the rather bulky 2-oxo-1,3-dioxolan-4-yl alkyl in **1** not only fits into the bottom (α) part of the corrin but is then part of a rather stable B_{12} alkyl.[43-45]

A more detailed consideration of the factors possibly involved in controlling α vs β isomers reveals that they are not well understood. In particular, it is poorly understood how the following affect the α/β ratio: the roles of kinetic vs thermodynamic control [e.g., in the oxidative addition of alkyl halides to Co(I) corrins]; the role of Co(I) or Co(II) corrin structures and conformations, for example in S_N2 or radical oxidative-addition mechanisms,[46] respectively (no Co^1-B_{12s} crystal structure is yet available); the role of steric effects; the role of electronic effects; the possible role

(41) (a) Finke, R. G.; Hay, B. P. *Inorg. Chem.* **1984**, *23*, 3041. (b) Hay, B. P.; Finke, R. G. *J. Am. Chem. Soc.* **1986**, *108*, 4820.

(42) (a) The photolysis of ethylcobalamin in small amounts of air (10^{-4} mmHg) produces ethylene but no appreciable butane or ethane: Dolphin, D.; Johnson, A. W.; Rodrigo, R.; Shaw, N. *Pure Appl. Chem.* **1963**, *7*, 539. (b) We considered O_2 capture of the 2-oxo-1,3-dioxolan-4-yl free radical, followed by a intramolecular β-H atom abstraction, and then a β-fission loss of $HO_2^{\bullet}$ to yield ethylene carbonate. However, the last step of this mechanism appears to be too endothermic to be viable and has little precedent within the radical literature to our knowledge. (c) Air-saturated H_2O contains 2.6×10^{-4} M O_2 at 25 °C: Gordon, A. J.; Ford, R. A. *The Chemists Companion*; John Wiley and Sons: New York, 1972; p 39.

(43) Compared to cyclopentylcobalamin whose $t_{1/2}$ = 3.1 min in pH 7 buffer,[17b] diastereomeric **1** is rather stable with no detectable change in 2 h [approximate half-lives for aerobic thermolysis of the individual diastereomers of **1** in unbuffered H_2O are 93 (α_2 isomer) and 250 h (α_1 isomer) at 40 °C; see the text for additional data].

(44) (a) The X-ray crystallographically determined structures of the individual diastereomers of **1** would be of interest; they will, however, require strongly diffracting crystals and the absence of the type of alkyl group disorder that we encountered previously (at least in a nonchiral, non-corrin B_{12} model).[19] Known corrin ring fluxionality,[44b] and comparison of **1** to the crystal structure of cyanocobalamin,[44c] suggest that the alkyl in α-**1** may adopt an orientation[45] similar to the imidazole moiety of cyanocobalamin, with the strong Co–C bond in α-**1** further forcing the corrin to bend upwards to accommodate the α-alkyl group. Such an upward conformational distortion or bending of the corrin in **1** is consistent with the steric requirement found in this work for β-axial nitrogenous-base binding. (b) Pett, V. B.; Liebman, M. N.; Murry-Rust, P.; Prasad, K.; Glusker, J. P. *J. Am. Chem. Soc.* **1987**, *109*, 3207-3215. (c) Glusker, J. P. In B_{12}; Dolphin, D., Ed.; Wiley-Interscience: New York, 1982; Vol. 1, p 32.

(45) Ethylene carbonate and chloroethylene carbonate have nonplanar, half-chair conformations: Pethrick, R. A.; Wilson, A. D. *Spectrochim. Acta* **1974**, *30A*, 1073-1080. Jaakko, P.; Sirkka, K. *Suom. Kemistil. B* **1970**, *43*, 285-288; *Chem. Abstr.* **1970**, *73*, 98111. Brown, C. *Acta Crystallogr.* **1954**, *7*, 92.

(46) (a) Collman, J. P.; Hegedus, L. S.; Norton, J. R.; Finke, R. G. *Principles and Applications of Organotransition Metal Chemistry*; University Science Books: Mill Valley, CA, 1987; Chapter 4. (b) Schrauzer, G. N.; Deutsch, E. *J. Am. Chem. Soc.* **1969**, *91*, 3341.

of β (and/or α) "blocking groups" such as H^+ or Zn^{2+} leading to possible β (or α) [H–Co] or β (or α) [Zn^{2+}–Co] complexes; and the conceivable role of α,β-dialkyl intermediates produced if strongly reducing conditions are present.

Brown has noted that thermodynamic control appears to predominate in small, electron withdrawing groups (relative to CH_3) such as CN^- or $HC{\equiv}C^-$.[22b,c] Specifically, the CN^- group prefers the α face of a Co(III) cobinamide over the β face by a factor of ~2:1 when the α-axial position is not blocked.[3] However, the addition of 1 equiv of CN^- to *base-on* B_{12a} leads only to β-cyanocobalamin.[3] This kinetically controlled case favoring the β isomer is presumably the expected result of employing a base-on, and thus α-face-blocked, cobalamin. Since photolysis converts α-**1** into the (thermodynamically more stable) β-**2**, this requires that **1** results from kinetic control when this alkylcobalamin is formed *under base-on conditions*. It rigorously says nothing, however, about the mechanism of formation of α-**1**, since the Zn/HOAc synthesis conditions involve *protonated, base-off* B_{12}. The addition of $HC{\equiv}C^-$ to aquocobinamide produces 1:1 α to β isomers;[9] the possibility of an electron-transfer mechanism, proceeding via a Co(II) intermediate, has not been ruled out in this case (and in fact seems likely).[47]

An interesting example that provides a strong case for kinetic control of the α/β ratio is the oxidative addition of either MeI or MeOTs to Co(I) heptamethylcobyrinate,[47] a corrin system where no appended (and thus no blocking) axial base is present (other than a possible THF from the THF/toluene solvent system). MeOTs addition, which is well-known to strongly prefer "$2e^-$", S_N2-like mechanisms with transition-metal nucleophiles,[46a] leads to mostly the β-Me product (75%). On the other hand MeI, which may undergo $1e^-$ mechanisms (although this is controversial)[46a] and thus could proceed via a Co(II) intermediate,[47b] gives essentially the opposite result, 73% α-Me and 7% of β-Me products for an α/β ratio[47a] of greater than 10:1! An alternative explanation, that these results simply reflect the different sizes or transition states for the two different alkylating groups both proceeding by a S_N2 mechanism, seems unlikely.

It is worth noting that α isomers are generally among the products obtained from acidic conditions when Zn is used as a reducing agent. Hence it must be considered that either a β-[H–Co] or a complex β-[Zn^{2+}–Co] is formed where the β face is blocked (thereby preferentially forming the α isomer), although it is not clear why an α face H–Co or Zn–Co complex would not also form (there are also other possibilities).[48] The possibility of a "H–Co(III)" species leads in turn to the unanswered question of just exactly what is the still poorly defined compound(s) known as "hydridocobalamin".[49]

One other conceivable mechanism is a "relay mechanism", where the α-axial benzimidazole is alkylated first by RX, followed by intramolecular nucleophilic displacement by cobalt leading to the α-Co alkyl (with the benzimidazole as the leaving group). This mechanism, unlikely from the start given the much greater nucleophilicity ("supernucleophilicity")[46b] of Co^1-B_{12s} vs the benzimidazole nitrogen, can be ruled out given the following control experiment (described in greater detail in the Experimental Section). Even at 2.7 times as concentrated as the conditions for the synthesis of **1**, chloroethylene carbonate plus 1,5,6-trimethylbenzimidazole in CD_3OD/NH_4Br showed little reaction (by ^1H NMR) over a time period (30 min) 6-fold longer than that required for the reaction of chloroethylene carbonate with Co^1-B_{12s}/Zn/MeOH. Hence, a relay mechanism such as described above can be ruled out.

Clearly, further investigations are needed to better understand the mechanisms leading to, and the factors influencing, α-alkyl- vs β-alkylcobalamins and -cobinamides. These should include the synthesis of a wider range of alkyls[8a] (whose electron-donating or -withdrawing ability and steric size vary systematically), determination of their α/β ratios under systematically controlled synthesis conditions, studies of kinetic vs thermodynamic control of the α/β ratio, and then kinetic and mechanistic studies of the most promising systems.

The biological role, if any, of α-alkylcorrins also remains to be established. Further studies of the possible role of α-methylcorrins in methyl transferase reactions are needed in this regard.[13]

Summary

In summary, the following are the major findings of the present study: (1) the synthesis of α-(2-oxo-1,3-dioxolan-4-yl)cobalamin (**1**), the first example of an α-alkylcobalamin containing a relatively bulky and electron withdrawing five-membered ring alkyl group, and the only example of an α-alkylcobalamin containing a chiral alkyl group; (2) unequivocal characterization of **1** by HPLC, FAB-MS, IR, and UV–visible spectroscopy, and 1- and 2-D NMR methods, making **1** the best characterized α-cobalamin presently known; (3) separation of **1** into its two diastereomers, and a comparison of the thermolysis rates of these two diastereomers; (4) studies of key physical properties of **1**, notably its β-face axial base binding constants, and the interesting photochemical conversion of **1** into **2**, the latter demonstrating that *base-off* **1** is a kinetic product relative to *base-on* **2**; (5) the important realization that α-alkylcobalamins may be more general products than has been previously appreciated in alkylcorrin syntheses involving alkyl groups with electron-withdrawing substituents, the α isomers possibly being lost in workups that employ (carboxymethyl)cellulose columns;[15] and (6) a discussion of what is and is not known about the mechanisms of formation and factors influencing α- vs β-alkylcorrin complexes and the possible role(s) of α-alkylcorrins in biology, discussion that should help guide further research in this area.

Experimental Section

Equipment. NMR spectra at Oregon were recorded on a General Electric QE-300 spectrometer. IR spectra were recorded on a Nicolet 5DXB FT-IR, using a matched pair of CaF_2 solution cells (International Crystals Inc). UV–visible spectra were taken on a Beckman DU-7 spectrometer and the data transferred to a Apple II Plus computer for storage. A Schlenk cuvette (a UV–visible cell with a Teflon needle valve glass blown onto its top) was used throughout for anaerobic reactions. FAB mass spectra were provided by the Oregon Microanalytical Lab (VG ZAB-2FHF mass spectrometer with a VG 11·250 data system). A vacuum atmospheric inert atmosphere (N_2) drybox containing less than 2 ppm O_2 was used for air-sensitive work. HPLC was performed on a Millipore Waters Model 510 HPLC equipped with a Lambda-Max Model 481 LC spectrophotometer and recorded on a Waters 740 data module. The columns used were an Alltech 300 mm × 4.1 mm Versapack C-18 as an analytical column, and a Hamilton 305 mm × 7 mm i.d. 10-μm particle size PRP-1 reversed-phase liquid chromatography semipreparative column. Twice-distilled H_2O was used during HPLC runs.

2-D NMR Spectroscopy. All of the 2-D NMR experiments were performed at Emory on a General Electric GN·500 spectrometer at room temperature (20 °C) without sample spinning. Care was taken to min-

(47) (a) Kräutler, B.; Caderas, C. *Helv. Chim. Acta* **1984**, *67*, 1981. (b) Kräutler postulates[47a] the possibility of a radical mechanism to account for his unusual MeI vs MeOTs results.

(48) (a) As detailed in the Experimental Section, a small effect on the α/β ratio (bigger than 1σ but not 2σ error bars) was discovered if the B_{12a}/Zn/HOAc solution is bubbled with drybox N_2 (releasing the H_2 pressure). Although additional studies are needed, this observation could be indicative of anything from α or β N_2 or H–H[48b] complexes [the latter presumably for Co(III) but not Co(I)],[48b] involvement in the oxidative-addition reaction[46a] of Co(II) (possibly oscillating)[48c] from a $2H\text{–}Co^{III} \rightleftharpoons 2Co^{II} + H\text{–}H$ equilibrium,[48c] or possibly even the role of residual H_2O in the HOAc or from the glassware, the water perhaps serving to deprotonate the acidic[49c] α or β $H\text{–}Co^{III} + H_2O \rightleftharpoons H_3O^+ + Co^1\text{-}B_{12a}$, thereby influencing the α/β ratio (?). (b) A d^6 M(porphyrin) (M = Os, Ru) forms a H–H complex: Collman, J. P.; Wagenknecht, P. S.; Hembre, R. T.; Lewis, N. S. *J. Am. Chem. Soc.* **1990**, *112*, 1294–1295, and references therein to the literature of H_2 complexes. (c) Chemaly, S. M.; Hasty, R. A.; Pratt, J. M. *J. Chem. Soc., Dalton Trans.* **1983**, 2223–2227. Note that this system is a gas evolution (H_2) chemical oscillator, one where the Co(II) concentration also oscillates.

(49) (a) Schrauzer, G. N.; Holland, R. J. *J. Am. Chem. Soc.* **1971**, *93*, 4060–4061. (b) Chemaly, S. M.; Pratt, J. M. *J. Chem. Soc., Dalton Trans.* **1984**, 595–599. (c) Lexa, D.; Savéant, J. M. *J. Chem. Soc., Chem. Commun.* **1975**, 872–874. These workers report a $pK_a = 1$ in H_2O for "hydridocobalamin", meaning that their species probably cannot be formed by protonation from HOAc ($pK_a = 4.7$) *in HOAc* (note the HOAc vs H_2O solvent difference, however). If formed some other way, such a strong acid could be stable in *absolutely dry* HOAc (H_2OAc^+ $pK_a = -6.5$) but not wet HOAc.

imize even transient exposure of α_1-**1** to room light (e.g., the room lights were turned off while the sample was loaded into the probe) after it was found that even a flashlight caused sample decomposition (see Handling of Light Sensitive Materials, vide infra), and after early attempts without rigorous light exclusion led to ca. 30% sample decomposition to Co^{III}-B_{12a}. Proton and carbon chemical shifts were referenced to internal trimethylsilyl propionate (TSP). All 2-D spectra were processed by using the FTNMR program (Hare Research, Inc., Woodinville, WA). All of the 2-D NMR experiments were performed on a sample containing 5.0 mg of the single diastereomer α_1-**1** in 0.5 mL of D_2O and having a pH of 7.8. The APT experiment was performed on a General Electric QE-300 spectrometer on a sample of the model compound,[19] (2-oxo-1,3-dioxolan-4-yl)Co[C_2(DO)(DOH)$_{pn}$]Cl, that was 0.1 M in DMSO-d_6.

HOHAHA Spectroscopy. The HOHAHA spectra resulted from a 512 × 1024 data matrix size with 16 scans per t_1 value. Delay time between scans was 1.0 s. An MLEV-17 mixing sequence of 105.9 or 10.6 ms preceded and followed by 2.0-ms trim pulses was used. Six watts of power provided a 60-ms 90° ^{1}H pulse width. A Gaussian function with a line broadening of −1 Hz and a Gaussian coefficient of 0.1 was used prior to Fourier transformation in the t_2 dimension. A cosine bell squared filter was used prior to Fourier transformation in the t_1 dimension.

Phase-Sensitive NOE Spectroscopy. The phase-sensitive NOE spectra resulted from a 512 × 2048 data matrix size with 16 scans per t_1 value. Presaturation of the residual HOD peak was used. Delay time between scans was 3 s and the mixing time was 500 ms. A Gaussian function with a line broadening of −1 Hz and a Gaussian coefficient of 0.1 was used prior to Fourier transformation in the t_2 dimension. A cosine bell squared filter was used prior to Fourier transformation in the t_1 dimension.

HMQC Spectroscopy. The one-bond ^{1}H–^{13}C shift correlation spectra resulted from a 256 × 1024 data matrix size with 192 scans per t_1 value (preceded by four dummy scans). Delay time between scans was 1.0 s. Forty-one watts of ^{13}C rf power and a 38-ms 90° pulse width were used. A combination of a Gaussian and a sine bell function was used prior to Fourier transformation in the t_2 dimension. A sine bell filter function was used prior to Fourier transformation in the t_1 dimension.

HMBC Spectroscopy. The multiple-bond ^{1}H–^{13}C shift correlation spectra resulted from a 256 × 1024 data matrix size with 272 scans (preceded by four dummy scans) per t_1 value and a delay time between scans of 1.0 s. Forty-one watts of power and a 38-ms 90° ^{13}C pulse width were used. Values of Δ_1 (the delay between the first 90° proton pulse and the first 90° ^{13}C pulse) and Δ_2 (the delay between the first and second 90° ^{13}C pulses) were 3.3 and 50 ms, respectively. In the t_2 and t_1 dimensions, a sine bell filter was used prior to Fourier transformation.

Materials. Solvents were used without purification unless indicated otherwise. The following were all from Baker unless noted otherwise: HPLC grade CH_3CN and MeOH; standard 0.1000 N NaOH and 0.1000 N HCl solutions; standard buffer solutions pH 7, pH 4, and pH 10; glacial acetic acid (used as received); as well as the NMR solvents D_2O and CD_3OD (Cambridge Isotope). House N_2 was purified through a U-tube-shaped glass system; one tube was a 20 in. × 1.5 in. column packed with Linde 4-Å molecular sieves, while the second 20 in. × 1.5 in. tube was a heated column packed with BASF R3-11 oxygen scavenger in a hydrogen reduced (black) form.

Several inorganic and organometallic chemicals were used as received: $H_2OB_{12}^+Cl^-$ (Sigma); NH_4Br (Matheson Coleman & Bell); Zn dust (oven-dried); and NH_4OAc (Baker). Chromatography materials used were CM-23 (carboxymethyl)cellulose fibrous (Whatman); Sephadex-SP C25 40-120 μm (Sigma); and XAD-2 absorbent particle size 0.125–0.15 μm (SERVA). Pyridine (Aldrich) and 1-methylimidazole (Aldrich) were each purified by distillation from CaH_2 before use; (±)-histidine (Aldrich) was used as received. Chloroethylene carbonate (Aldrich) was vacuum distilled to a clear liquid (n_D^{20} = 1.4540).[16b] 1,5,6-Trimethylbenzimidazole was prepared by the literature method[50a] [mp 143–144 °C (lit.[50a] mp 142–143 °C]. TEMPO was purified by room-temperature sublimation under reduced pressure [20 mmHg, mp 39 °C (lit.[41] mp 36–38 °C)].

Handling of Light-Sensitive Materials. Alkylcobalamins are generally very light sensitive, with secondary alkylcobalamins extremely so.[17b] Exposure of dilute solutions of alkylcobalamin to even diffuse room light causes cleavage of their Co–C bond; hence, special caution is required to avoid any exposure to light when these compounds are handled. Transfer and chromatography of light-sensitive solutions was accomplished either in a dark room or in a darkened hood (a fume hood shrouded with a black plastic curtain). A photosafe 5-W red light was used throughout. All glassware used in the darkened hood or darkroom, including the chromatography column, was shielded from the red light by aluminum foil to minimize any decomposition under even these dim lighting conditions.

The extreme photosensitivity of the α_1-**1** and α_2-**1** diastereomers, and thus the importance of minimizing their exposure to *the light of even an AA flshlight*, were probed in a control experiment. Two separate cuvettes (ca. 1 × 10^{-4} M solutions), one for each diastereomer, were prepared in a darkroom under air and were then individually exposed in an otherwise dark room to the light from an AA cell flashlight held with its lens directly against the cuvette. The subsequent aerobic photodecomposition was followed by visible spectroscopy. (Stray-light-induced decomposition, or decomposition within the light beam of the instrument, was considered as potential problems with these experiments. These were judged *not* to be a problem for the following reasons, respectively: UV–visible data were reproducible, and the amount of time in the spectrophotometer did not influence the results.) Overlaid spectral plots exhibited clean isosbestic points at 341 and 508 nm. Decomposition half-lives are 90 ± 10 for α_1-**1** and 60 ± 10 s for α_2-**1**. These results are reproducible as long as the flashlight is placed in the same way every time and if the samples fit entirely within the beam of the flashlight.

Determination of the Concentrations and the Extinction Coefficients of Alkylcobalamins. Extinction coefficients of **1** and **2** in aqueous solution were determined from the aerobic photolysis of the alkylcobalamin in the presence of KCN, since dicyanocobalamin has the highest, well-known extinction coefficient of all known cobalamins.[50b] The value of ϵ = 3.04 × 10^4 cm^{-1} M^{-1} (for the γ band between 350 and 360 nm) determined in deionized H_2O is commonly used as a reference.[50b] The extinction coefficients of the alkylcobalamins were then calculated according to $\epsilon_l = A_l/C_x$.

Synthesis of α-(2-Oxo-1,3-dioxolan-4-yl)cobalamin in MeOH with Zn/NH_4Br. In the drybox, 20 mL of *fresh* MeOH (UV grade) was added to a 50-mL septum-capped round-bottom flask containing 0.5 g (0.36 mmol) of $H_2OB_{12}^+Cl^-$, 1.0 g (10.2 mmol) of NH_4Br, and a stir bar. When the solids were fully dissolved, 2.0 g (30.6 mmol, 85 equiv) of activated Zn dust (oven-dried by baking it in a 160–200 °C oven under air overnight)[17] was added, producing a heterogeneous reaction mixture. Upon stirring this slurry, the color changed from red-brown to black. The solution was bubbled three times with box atmosphere to remove any H_2 generated (the bubbling was accomplished with one needle connected via hose to an external vacuum pump, and a second needle immersed into solution as the bubbler). With additional stirring (ca. 10 min), the color changed from black to greenish black, indicating the formation of Co^I-B_{12s}. The flask was wrapped with foil to protect the solution from light. Colorless chloroethylene carbonate (200 μL, 2.46 mmol, 7.2 equiv; freshly distilled if it is not colorless) was then added and the solution was purged with box atmosphere three times to further remove any H_2 generated. After ca. 5–10 min, the foil-wrapped, septum-capped flask was removed from the box and brought into a darkroom for workup.

In a darkroom, the solution was rapidly filtered through a 15-mL medium frit to remove Zn and poured into a 250-mL separatory funnel containing 100 mL of 0.01 M KH_2PO_4 solution, pH ca. 5.2. This mildly acidic pH ensures that the base-sensitive, carbonate-containing alkyl in **1** remains intact. Some protonated **1**·H^+ (pK_a 5.4) but only *un*protonated **2** are formed (the pK_a of **2**·H^+ is[16b] 2.2), thereby aiding their separation by cation-exchange chromatography. (The total elapsed time from the addition of the chloroethylene carbonate until the removal of the excess Zn should be no more that 10–15 min to avoid Zn reductive cleavage of the Co–C bond.[16d]) Excess alkylating reagent was removed by twice extracting (50 mL) with ether. Ether dissolved in the aqueous phase was removed by rotary evaporation at 25 °C. At this point there appeared to be something suspended in the solution, so it was vacuum filtered through Whatman No. 1 paper on a Büchner funnel. [The transparent wax-like material, recovered from the filter paper and presumably a polymer such as poly(vinylene carbonate) from the chloroethylene carbonate precursor, was not identified.] The filtered solution was desalted on a 9 cm long × 3.5 cm i.d. XAD-2 column, by first washing the column with deionized H_2O until the eluent was free from salt (determined by $AgNO_3$ titration), followed by eluting the cobalamin with 50%/50% (v/v) CH_3CN/H_2O. The desalted mixture in CH_3CN/H_2O was reduced to ca. 20 mL on rotary evaporation, keeping the temperature of the water bath at <25 °C to avoid thermolysis of the relatively weak Co–C bond. The concentrated solution was then loaded onto a 30 cm long × 2 cm i.d. CM-23 cellulose cation-exchange column. Cobalamin **2**, β-(2-oxo-1,3-dioxolan-4-yl)cobalamin (as its mixture of two diastereomers), was eluted by deionized H_2O. Removal of solvent by rotary evaporation and freeze-drying yielded 117 mg (23%) of **2** as a red powder: ^{1}H NMR (0.7 M DCl in D_2O, vs HOD impurity, downfield region only; the full spectrum is available as Figure I, supplementary material) δ 6.32 (d, 1 H, R1), 6.75 and 6.72 (s, 1 H, C10), 7.30 (s, 1 H, B4 or B7), 7.36 (s, 1 H, B4 or B7), 8.97 (s, 1 H, B2); HPLC (analytical column, flow rate, 1 mL/min) using 25% CH_3CN/75% 0.01 M KH_2PO_4 buffer, 5.48 min (1

(50) (a) Simonov, A. M.; Pozharskii, A. E.; Marianovskii, V. M. *Ind. J. Chem.* **1967**, *5*, 81. (b) Hill, H. A. O.; Pratt, J. M.; William, S. *Proc. R. Soc.* **1965**, *A288*, 362.

peak); using 25% MeOH/75% 0.01 M KH_2PO_4 buffer, 43.37 and 58.09 min (two peaks due to two diastereomers, 52%/48%); UV-visible (H_2O, ϵ (cm^{-1} M^{-1})) 527 nm (9.2×10^3), 368 (1.43×10^4), 338 (1.55×10^4); (0.2 N HCl) 458, 397, 320.5; IR $\nu_{C=O}$ (carbonate group; KBr) 1795, 1775, 1665 (strong; B_{12} amide carbonyls); $\nu_{C=O}$ (carbonate group; in MeOH) 1800, 1770, and ca. 1650–1675 cm^{-1} (strong; B_{12} amide carbonyls); FAB-MS (*m*-nitrobenzyl alcohol matrix, low resolution) calcd molecular mass for $\{C_{65}H_{91}O_{17}N_{13}PCo\}\cdot H^+$ 1416.58, found *m/e* $(M + H)^+$ 1416.6.

Compound **1** (as a mixture of its two diastereomers) and Co^{III}-B_{12a} were removed from the CM-23 column by eluting with 0.02 M NaCl. The volume of the solution was reduced to ca. 15 mL by rotary evaporation and the solution was loaded onto a 35 cm long × 3.5 cm i.d. Sephadex-SP C-25 cation-exchange column. The column was washed with ca. 250 mL of deionized H_2O to remove any cobalamin **2** that might be remaining and then eluted with 0.2 M NaCl in order to separate **1** and B_{12a}. Twnety 15-mL fractions were collected. The first 13 fractions contained only **1** as determined by UV-visible spectroscopy. Fractions 14–20, which contained trace B_{12a}, were combined and desalted via the XAD-2 column and rechromatographed on the Sephadex-SP column, this time with 0.1 M NaCl as the eluent. The eluent containing **1** from both Sephadex-SP column separation were combined and desalted on an XAD-2 column as described above; this step apparently also deprotonates any remaining $\mathbf{1}\cdot H^+$. CH_3CN of the resulting solution was removed by rotary evaporation at room temperature. Finally, H_2O was removed by freeze-drying to produce α-(2-oxo-1,3-dioxolan-4-yl)cobalamin (**1**) as an orange-red powder, yielding 88 mg (17%): ^1H NMR (D_2O plus 0.7 M DCl, vs HOD impurity, downfield region only) δ 6.28 (d, 1 H), 6.36 (d, 1 H), 7.35 (d, 1 H), 7.42 (d, 1 H), 9.02 (d, 1 H); ^1H NMR (neutral D_2O) δ 6.25 (d, 1 H), 6.39 (d, 1 H), 7.26 (d, 1 H), 7.34 (d, 1 H) 8.31 (d, 1 H); HPLC (analytical column, flow rate, 1 mL/min) using 25% CH_3CN/75% 0.01 M NH_4OAc buffer, 5.5 min (1 peak); (preparative column) 20% CH_3CN/80% H_2O, 11 and 13 min (two peaks due to two diastereomers, 55 ± 5% to 45 ± 5% ratio); IR (carbonate group; KBr) $\nu_{C=O}$ 1795, 1775, 1665 (strong; B_{12} amide carbonyls); (MeOH) $\nu_{C=O}$ 1800, 1776, 1665 cm^{-1}; UV-visible (H_2O, ϵ(cm^{-1} M^{-1})) 324.0 nm (1.920×10^4), 483.5 (1.025×10^4); FAB-MS (*m*-nitrobenzyl alcohol matrix, low resolution) calcd molecular mass for $\{C_{65}H_{91}O_{17}N_{13}PCo\}\cdot H^+$ 1416.58, found *m/e* 1416.7 ($[M + H]^+$), 1329.7 ($[M + H - alkyl]^+$). Note that the β-axial ligand, presumably H_2O, is not seen in the FAB-MS [the β-axial ligand apparently being lost during the desorption process, as we have previously observed[51] for an α-axial H_2O in adenosylcobinamide·$(H_2O)^+X^-$]. Other fragment peaks are consistent with the literature.[52]

Subsequent attempts to repeat the above MeOH/Zn/NH_4Br method, but on $^1/_2$ scale (250 mg; one run) to $^1/_4$ scale (125 mg; eight runs) of $(H_2O)B_{12}{}^+Cl^-$, by one of us who had no prior experience with this preparation, gave comparable yields of 14–23% **α-1**, 21–28% **β-2**, and 24–45% Co^{III}-B_{12a} in five of the nine runs. However, in the four other experiments [125-mg scale of $(H_2O)B_{12}{}^+Cl^-$] the yields were noticeably lower, 2–8% **α-1**, 2–10% **β-2**, and 75–85% of apparently unreacted B_{12a} by HPLC. Moreover, the α/β ratio was somewhat variable, ranging from 0.6 to 1.2, throughout all nine experiments (i.e., even in the five experiments that gave 14–23% **1**). We suspect, but have not proven, that the source of these variable results is the extreme light sensitivity of these materials (vide infra), plus perhaps the need to gain some experience and practice with this preparation.

While additional experiments might provide useful insights into the cause(s) of the variable yields and α/β ratio, a search for a more reliable preparation was deemed a higher priority and was in fact successful. Specifically, the Zn/HOAc method given below, plus a different workup consisting of preparative HPLC, provided a very reproducible synthesis with a reproducible α/β ratio and separated, pure diastereomers of **1** in milligram quantities.

Synthesis of α-(2-Oxo-1,3-dioxolan-4-yl)cobalamin, the Zn/HOAc Route, and Separation of the α_1-1 and α_2-1 Diastereomers. In the drybox, 20 mL of deoxygenated glacial acetic acid (undried;[48a] used as received) was added to a 50-mL round-bottom flask containing 500 mg (0.36 mmol) of $(H_2O)B_{12}{}^+Cl^-$, 2.0 g (30.6 mmol, 85 equiv) of oven-dried Zn, and a stir bar. The flask was capped with a rubber septum (a pressure buildup results presumably from H_2 formed by Zn reduction of H^+ from acetic acid); *bubbling with box N_2 was not employed as part of the experiment* (but it was as part of later experiments, vide infra). Stirring was carried out for 10 min until the solution was dark green, indicating complete reduction of the $Co^{III}(H_2O)B_{12a}{}^+Cl^-$. The flask was wrapped with aluminum foil and 200 μL (2.46 mmol, 7.2 equiv) of colorless (or freshly distilled) chloroethylene carbontae was added via syringe. Stirring was continued for 3 min and the flask was then removed from the box and taken into the darkroom for workup. Zn was removed by filtration through a 15-mL medium frit. The filtrate was then poured into a 1-L separatory funnel containing 800 mL of diethyl ether, causing the cobalamins to precipitate. Everything else, including the Zn salts, remained in solution. (The total elapsed time to this point since the addition of chloroethylene carbonate should not exceed 10–15 min to avoid Zn reductive cleavage of the product's Co–C bond.) The crude solid, containing *protonated* $\mathbf{1}\cdot H^+$ and **2**, was collected by vacuum filtration in a 150-mL glass-fritted funnel, washed with 4 × 100 mL of ether, and then scraped into a flask where the last traces of ether were removed under 0.01 mmHg vacuum. This procedure, repeated twice on the 500-mg $(H_2O)B_{12}{}^+Cl^-$ scale, was also successfully run six times on a 250-mg $(H_2O)B_{12}{}^+Cl^-$ scale. The HPLC yield of **1** in all eight runs was 24–28% and of **2** 40–47% (Determined at 280 nm where **1**, **2**, and B_{12a} have equal ϵ values).

With the need to separate the diastereomers of the α isomer apparent, the ion-exchange purification procedures described above for the Zn/MeOH/$NH_4{}^+Br^-$ synthesis were abandoned in favor of preparative HPLC. The solids resulting from the ether precipitation were dissolved in distilled water (10 mL). This solution was filtered through 0.4-μm HPLC filters and then injected 1.5 mL at a time onto a Hamilton PRP-1 HPLC column. Conditions: isocratic at 14% CH_3CN/86% H_2O, flow rate 2 mL/min. Retention times: about 65 and 80 min for the first and second diastereomers, respectively. Peaks corresponding to α_1-**1** and α_2-**1** were collected in separate black tape and foil wrapped flasks, the CH_3CN was removed by rotary evaporation at room temperature, and the water was removed by freeze-drying to yield the separated diastereomers as a fluffy orange-red powder. Milligram yields of reasonably pure material are produced by this method. [No attempt was made to calculate the exact yields, which are low, in part due to incomplete collection of the HPLC peaks (peak tails were deliberately not collected so as to maximize the absolute purity of the material collected), and in part due to simple mechanical losses when dilute samples were freeze-dried (the sample adheres to the flask walls).]

HPLC retention times of the pure α_1-**1** and α_2-**1** diastereomers on the C-18 analytical column were identical with those of the original mixture of diastereomers. For α_1-**1**: ^1H NMR (D_2O vs HOD impurity; downfield region only) δ 6.25 (d, 1 H), 6.39 (s, 1 H), 7.26 (s, 1 H), 7.34 (s, 1 H), 8.31 (s, 1 H). For α_2-**1**: ^1H NMR (D_2O vs HOD impurity; downfield region only) δ 6.21 (br s or d, 1 H), 6.35 (s, 1 H), 7.29 (s, 1 H), 7.36 (s, 1 H), 8.23 (s, 1 H); an overlay of the spectra of the separated diastereomers in terms of the peak positions looks identical with the spectrum of the mixture at the same pH (the peak heights of course depend on the actual molar ratio of the two diastereomers present).

Note that the ^1H NMR clearly shows that the axial benzimidazole *is not* protonated in the α_1-**1** and α_2-**1** so obtained, despite the fact that diastereomeric $\mathbf{1}\cdot H^+$ is loaded onto the HPLC column. We surmise that the protonated axial 5,6-dimethylbenzimidazole is subsequently deprotonated during the preparative HPLC step, the much greater solubility/partitioning of neutral **1** (vs ionic $\mathbf{1}\text{-}H^+X^-$) in the C-18 phase of the HPLC column effectively making $\mathbf{1}\text{-}H^+X^-$ more acidic so that it is deprotonated by the neutral-water HPLC eluent (an expected effect, one presumably seen previously in other HPLC work).[53]

The N_2 Bubbling/H_2 Pressure Effect. In the course of refining the Zn/HOAc synthesis we noticed that the α to β isomer distribution changes *slightly* depending on whether or not the reaction mixture is bubbled with box atmosphere (dry N_2) during the reduction of B_{12a} by Zn in HOAc. This bubbling procedure was initially instituted to remove a H_2 pressure buildup (also noted by others;[49b] due to Zn reduction of H^+). In order to get a good estimate of the α/β isomer distribution, the above Zn/HOAc synthesis was subsequently repeated eight times on a 125-mg scale. In the first four runs, the experiment was done without N_2 bubbling and with a H_2 pressure buildup in the septum-capped flask as described above. In the second set of four experiments, the reaction mixture was bubbled with the box, dry N_2 atmosphere (the bubbling was accomplished as described for the Zn/MeOH/NH_4Br synthesis). The reaction mixtures were analyzed by HPLC and the average α/β ratios (and 1σ error bars) computed for the four reactions of each set. The results indicated an α/β ratio of 0.50 ± 0.05 with no bubbling and 0.63 ± 0.03 when bubbling was carried out, or 0.56 ± 0.08 (taken to be 0.6 ± 0.1) under all conditions examined. Note that the difference is more than the stated 1σ error limits, but is not significant at 2σ error limits. This unexpected observation of a small, *possibly* real effect due to this N_2 bubbling/H_2 pressure removal step can be rationalized[48,49] and may

(51) Hay, B. P.; Finke, R. G. *J. Am. Chem. Soc.* **1987**, *109*, 8012.

(52) (a) Barber, M.; Bordoli, R. S.; Sedgwich, R. D.; Tyler, A. N. *Biomed. Mass Spectrom.* **1981**, *8*, 492. (b) Amster, I. J.; McLafferty, F. W. *Anal. Chem.* **1985**, *57*, 1208.

(53) Our efforts to locate a reference to such an effect in the HPLC literature failed, although we suspect that such an effect has been seen previously.

be worthy of further study, especially the following: additional, more precise data; studies of Ar (rather than N_2) bubbling (i.e., is this effect still seen?); is the ratio influenced by the amount of H_2O impurity present if, say, the HOAc and glassware used are carefully dried (or does bubbling with dry N_2 change the acetic acid's H_2O content?) Note that undried HOAc (glacial, used as received, probably wet) was used throughout these Zn/HOAc experiments since the N_2 bubbling effect was discovered only late in these studies.[48,49]

Chromatography Column Preparations. CM-23 Cation-Exchange Column. In a 1000-mL beaker, 20 g (wet volume 300 mL) of CM-23 cellulose (Whatman) was soaked in 600 mL of 0.5 N NaOH for 80 min and washed with distilled H_2O until the pH of the wash was near neutral (pH 8). The cellulose was then soaked in 600 mL of 0.5 N HCl for 30 min and washed with distilled H_2O until neutral. The prepared cellulose was loaded into a 30 cm long × 2 cm i.d. column. Before each use, this column was washed with eluent until the column reached equilibrium, as determined by testing the eluent with pH test paper. After each use, the column was regenerated by washing first with 0.1 N HCl and then with distilled H_2O until neutral.

Sephadex-SP Column. In a 1000-mL beaker, 60 g (wet volume 400 mL) of Sephadex-SP C25 was soaked in 700 mL of distilled H_2O for 24 h. The top solution was decanted and the remaining material washed with H_2O five times. The resulting Sephadex was loaded into a 35 cm long × 4 cm i.d. column and then washed with 2 N NaCl, shrinking the bed to two-thirds of its original volume. The column was washed with H_2O until the eluent was Cl^--free (by $AgNO_3$ titration), causing the Sephadex to reexpand to its original volume. After each use, the column was regenerated by washing with 2 N NaCl (and, if necessary, with 0.005 N NaOH to remove B_{12a}) followed by washing with H_2O until the eluent was Cl^--free.

XAD-2 Column. In a 500-mL beaker, 55 g of XAD-2 (wet volume 150 mL) was soaked in 200 mL of 50% CH_3CN/50% H_2O mixed solvent. When foaming had ceased, the resin was poured into a 9 cm long × 3.5 cm i.d. column. The column was washed with distilled H_2O until the eluent was CH_3CN-free as tested by a wet pH test paper. After each use, the column was washed with 50% CH_3CN/50% H_2O until the eluent was colorless and then with distilled H_2O to regenerate the column.

Yield of 1 and 2 vs Equivalents of Zn. Following the literature procedure,[17b] $(H_2O)B_{12}{}^+Cl^-$ (28.62 mg, 0.0207 mmol) and oven-dried (>160 °C) Zn dust (26.41 mg, 0.404 mmol) were weighed directly and separately into two 8 mm × 72 mm test tubes and brought into the drybox. In the box, 1 mL of glacial acetic acid (undried, used as received) was added via gas-tight syringe to the tube containing B_{12a}. After the B_{12a} was completely dissolved by shaking and bubbling with box atmosphere three times, the red solution was transferred to the tube containing Zn via a gas-tight syringe. Again the solution was shaken and bubbled (vide supra) with box atmosphere several times. The color of the solution changed from red to brown and then to green (the color of Co^I-B_{12a}) in 10 min. Chloroethylene carbonate (50 mL, 0.61 mmol) was added to the greenish solution and the mixture was shaken and bubbled with box atmosphere three times. The foil-wrapped tube was then brought out of box.

In the darkroom, the solution was filtered through a 2-mL frit to remove Zn dust. The filtrate was diluted with 50 mL of freshly distilled dry ether. No more than 10–15 min had elapsed since the addition of chloroethylene carbonate to this point (i.e., the reaction was kept constant, so that only the total Zn surface area was changing). The cobalamin precipitate was centrifuged and washed with ether three times. The last trace of ether was removed under vacuum (<1 mmHg). The organe solid of the reaction mixture was dissolved in H_2O and subjected to HPLC analysis (Versapak analytical, reversed-phase C-18 column, isocratic 25% CH_3CN/75% 0.01 M NH_4OAc; 1 mL/min flow rate; 10 mL, λ = 280 nm). The retention times for **2**, **1**, and B_{12a} are 4.8 and 5.3 (for the two β diastereomers), 8.2, and 13.4 min, respectively.

The entire process was repeated four more times, each time with different amounts of Zn. The results of HPLC analysis of the final solids are summarized in Table IV.

Determination of Axial Base Equilibrium Binding Constant. To a H_2O solution of **1** (1×10^{-4}–5×10^{-5} M) was added a known amount of N-base [pyridine, 1-methylimidazole, or (±)-histidine]. A UV–visible spectrum was recorded. The concentration of each solution was corrected (for dilution by the added axial base) so as to retain the isosbestic points. The equilibrium constant was calculated according to Drago[54] or the plot of $A_{485.5}$ vs $(A_0 - A_{483.5})/[\text{base}]$, the slope of which equals $1/K_{eq}$, and intercept equals A_∞.[55] The binding for 1,5,6-trimethylbenzimidazole (Me_3Bz) was determined in methanol as described above (due to the insolubility of Me_3Bz in H_2O). A plot of $A_{483.5}$ vs concentration of base was used to evaluate the extent of base binding.

Table IV. HPLC Results of the Synthesis vs Equivalent of Zn

	reaction no.				
	1	2	3	4	5
B_{12a}					
wt, mg	25.52	25.06	26.24	28.62	27.20
mmol (×10⁻²)	1.85	1.82	1.90	2.07	1.97
Zn					
wt, mg	1.24	6.03	12.28	26.41	103.7
mmol (×10⁻²)	1.90	9.32	18.79	40.40	158.6
equiv vs B_{12a}	1.03	5.14	9.90	19.52	80.6
R-Cl					
vol, μL	50	50	50	50	50
mmol	0.61	0.61	0.61	0.61	0.61
HPLC[a]					
2%	12.4	28.9	37.6	40.1	38.3
1%	1.8	20.2	27.9	28.4	28.2
B_{12a}%	85.8	50.9	34.5	31.5	33.5

[a] Yields at 280 nm, where the ε coefficients for **1**, **2**, and B_{12a} are equal within experimental error.

Chart I

For a reaction $D + E \underset{}{\overset{K_{eq}}{\rightleftharpoons}} DE$

$$K_{eq} = \frac{[DE]}{([D]_0 \cdot [DE])([E]_0 \cdot [DE])}$$

assuming $[E]_0 >> [DE]$ ie. [base] >> [cobalamin]

$$K_{eq} = \frac{[DE]}{([D]_0 \cdot [DE])[E]_0}$$

$$\because\ A = \varepsilon_D b[D] + \varepsilon_{DE} b[DE]$$

$$[D] = [D]_0 \cdot [DE] \quad [D]_0 = [DE]_\infty$$

$$A_0 = \varepsilon_D b[D]_0 \quad A_\infty = \varepsilon_{DE} b[DE]_\infty$$

$$\therefore\ K_{eq} = \cdot \frac{A \cdot A_0}{A \cdot A_\infty} \cdot \frac{1}{[E]_0}$$

$$\therefore\ A = \frac{A_0 \cdot A}{[E]_0} \cdot \frac{1}{K_{eq}} + A_\infty$$

Axial Base pK_a Titration for α_1-1 and α_2-1. These titrations were carried out in 5-mm NMR tubes. Samples were prepared by dissolving 1–3 mg of cobalamin in 0.5 mL of D_2O. The initial pH(apparent) values are ca. 9–10 [pH(apparent = pH meter reading) = pD − 0.4].[56] Spectra were recorded at various pH(apparent) values as 2-mL aliquots of a dilute solution of DCl in D_2O were added to bring the pH(apparent) down to ~3. Titration curves (Figure J, supplementary material) were obtained by plotting the chemical shift of the protonation-sensitive B2 proton of the benzimidazole base as a function of the pH(apparent). The pK_a(apparent) values were the same for both α_1-**1** and α_2-**1**, 5.4 ± 0.3, and can be taken as reasonable initial estimates of the true pK_a values given the control described below (and with the added assumption that the D_2O vs H_2O isotope effect on the chemical shift of the B2 proton is either small or the same for α_1-**1** and benzimidazole-protonated α_1-**1**·H^+).

A simple control experiment was done to demonstrate the relationship between the pK_a(apparent) values so determined (i.e., for D^+ addition to the axial base in D_2O, but with the pH(apparent) measured by a H^+/H_2O calibrated pH meter) and the true pK_a values. The control experiment was a classical titration of 1-methylimidazole in H_2O and then in D_2O using a pH meter (calibrated in H_2O) vs the volume of added HCl or DCl, respectively, carried out as follows: approximately 0.2 g of 1-methylimidazole was dissolved in 10 mL of either H_2O or D_2O. The pH of the solution was measured (using a pH meter, Corning Model 125, equipped with an Omega Model PHE-2754 electrode, the same equipment used in the NMR titrations) at intervals as 0.4 M HCl in H_2O (or DCl in D_2O) was added. Classical titration curves were obtained by plotting pH vs the amount of acid added and the pK_a values determined from the inflection points of the titration curves. Comparison of the curves obtained in this way showed that the pK_a measured in H_2O was

(54) Drago, R. S. *Physical Method in Chemistry*; W. B. Saunders Co.: Philadelphia, PA, 1977; p 90.

(55) The linear plot of A vs $(A_0 - A)/[E]_0$ is derived as shown in Chart I. For the definition of each variable, see ref 54.

(56) (a) The pH(apparent = meter reading) in D_2O is related to the (better defined) pD (i.e., the well-defined reaction *in* D_2O, base + $D^+ \rightleftharpoons$ base-D^+) by the equation pH(apparent = that measured in D_2O) = pD − 0.4: Glasoe, P. K.; Long, F. A. *J. Phys. Chem.* **1960**, *64*, 188. The pK_a values for 1-methylimidazole measured this way, pK_a(apparent, in D_2O), were shown to be equal[56b] (±0.2 error bars) to the desired pK_a values (in H_2O); see the Experimental Section. (b) A literature reference demonstrating that pK_a(apparent, in D_2O) = pK_a(in H_2O) is: Roberts, G. C. K.; Meadows, D. H.; Jardetzky, O. *Biochemistry* **1969**, *8*, 2053 (see p 2054).

the same within experimental error (±0.2) as the pK_a(apparent) measured in D_2O, both values being 7.2 ± 0.2. This experiment shows that the pH(apparent) and pK_a(apparent) for the B_{12} compounds titrated can be taken to be equivalent to the true pH and true pK_a for the purposes (and stated ±0.3 error bars) of this work. Literature substantiating this point is available.[56b]

Thermolysis of the α_1-1 and α_2-1 Diastereomers. Samples for the thermolyses were taken directly from the HPLC column, as H_2O/CH_3CN solutions initially, in order to ensure that they were as pure as possible (the CH_3CN was then removed by rotovapping at 25 °C and 15 mmHg for 30 min). Samples of both diastereomers were then thermolyzed concurrently in the resultant unbuffered H_2O in order to ensure identical conditions. The solutions (approximately 1×10^{-4} M) were loaded into cuvettes in a darkroom (under air) and capped with rubber septa in order to prevent evaporation of the solvent during the thermolyses. They were then placed in the heated cell holder of a Beckman DU-7 spectrometer, where they were allowed to sit for 20 min to reach the thermolysis temperature prior to recording the first spectra. (No stirring was carried out.) Spectra were recorded at intervals of time, and a final spectrum (taken to be the infinity point) was recorded after photolysis of the solution with a 275-W sunlamp for 10 min. Overlay plots of the spectra exhibited rough isosbestic points at about 371 and 512 nm.

The resultant data were analyzed by recording the absorbance (A) for Co(III) appearance at 350.5 nm as a function of time and plotting ln $[(A_t - A_\infty)/(A_0 - A_\infty)]$ vs time, with k equaling the slope and $t_{1/2} = 0.693/k$. Error bars quoted are one standard deviation of the slope; the results were repeatable within the stated error limits. The ln plots were only reasonably linear (R = 0.95–0.98), but second-order and half-order plots were much worse (nonlinear).

The thermolyses were initially done at 40 ± 0.5 °C in order to mimic conditions that might be encountered during removal of solvent on the rotory evaporator. The half-lives were surprisingly long at this temperature; hence subsequent thermolyses were carried out at 53.7 ± 0.5 °C. Three runs at this temperature all gave the same results within experimental error.

Aerobic Photolysis of 1. Aerobic photolyses of **1** in pH 7 phosphate buffer were carried out by placing the solution ca. 40 cm from a 275-W sunlamp. No additional provision for cooling, other than from the air, was made since the solutions did not warm to the touch. Different concentrations of **1** were required by the different monitoring methods [$(4 - 10) \times 10^{-5}$ M for UV–visible studies, 7×10^{-3} for ^{1}H NMR, and 1×10^{-3} for FT-IR work]. Given that only the first of the above concentrations is lower than the 2.5×10^{-4} M solubility of 0.2 atm O_2 (air) in 25 °C (unbuffered) H_2O,[42b] and given the fact that all the solutions were not stirred (i.e., conditions of slow O_2 diffusion into solution) and were in sealed vessels in these initial survey experiments, substoichiometric O_2 is one key[42] to the vinylene carbonate product observed by IR and NMR (i.e., in the *higher* concentration experiments with **1**). Such "aerobic" photolyses of **1** produces the following: B_{12a} (isosbestic points at 342, 372, and 527 nm) *at UV–visible concentrations*, and vinylene carbonate, 70 ± 10% (7.4 ppm; two characteristic IR peaks at 1803 and 1835 cm^{-1}), *in separate ^{1}H NMR and IR experiments at higher concentrations*, plus presumably other undetermined organic and O_2-derived products.

Anaerobic Photolysis of 1 without and with TEMPO. A solution of **1** (ca. 5×10^{-5} M in deionized H_2O) was prepared in the drybox in a Pyrex cuvette, removed from the box, and then photolyzed with a 275-W sunlamp placed 40 cm from the cuvette for 70 s. UV–visible spectroscopy showed that a mixture of **2** plus Co^{II}-B_{12r} had been formed. Air oxidation of the solution and then HPLC analysis (PRP-1 reversed-phase column, 20% CH_3CN/80% H_2O; detecting wavelength 254 nm; 1 mL/min flow rate) showed 82% **2** and 18% Co^{III}-B_{12a}.

Anaerobic photolysis of **1** in the presence of TEMPO (200 equiv) was accomplished similarly. After 20 s of 275-W sunlamp photolysis at a distance of 40 cm, UV–visible analysis showed primarily Co^{II}-B_{12r}. After 75 additional s (95 s total) of photolysis, UV–visible spectra showed Co^{III}-B_{12a} and CO^{II}-B_{12r} (isosbestic points at 343, 374, 517 nm). Air oxidation and HPLC analysis as above showed 89% Co^{III}-B_{12a}, 11% α-**1**, but no detectable β-**2**.

Carbonate Deprotection and Subsequent Decomposition of 1 in pH 10 Borate Buffer. An aerobic solution of **1** in pH 10 borate buffer (5×10^{-4} M) was prepared in the dark. The thermal decomposition of **1** at 22 °C was followed by UV–visible spectroscopy for 13 h ($t_{1/2} \sim 3.5$ h). Then the solution was photolyzed with a 350-W sunlamp for 20 min to get the A_∞ value. The product of this reaction is B_{12a}, and the conversion has isosbestic points at 347.0, 374, and 511.5 nm. The first-order rate constant calculated from ln $[(A_t - A_\infty)/(A_0 - A_\infty)]$ at 357 nm (the formation of B_{12a}) gave $k_{obs} = 4.7 \times 10^{-5}$ s^{-1}.

Control Experiment Testing the Possibility of a Relay Mechanism in the Synthesis of α-1. In order to test the possibility that α-**1** is formed by a mechanism involving chloroethylene carbonate alkylation of the benzimidazole base N3 nitrogen, followed by attack of Co^I-B_{12s} on the chloroethylene carbonate (with displacement of the 1,5,6-trimethylbenzimidazole base), chloroethylene carbonate was added to 1,5,6-trimethylbenzimidazole (used here as a model of the axial base in B_{12}) under conditions designed to simulate those of the synthesis of α-**1**.

The following experiment was repeated twice using two different concentrations of chloroethylene carbonate. In the first trial, NH_4Br (17 mg, 0.15 mmol) was added to 1 mL of CD_3OD in a 5-mm NMR tube. 1,5,6-Trimethylbenzimidazole (8 mg, 0.05 mmol) was then added, giving a solution 0.05 M in this compound (2.7 times as concentrated as the reaction being modeled). A ^{1}H NMR spectrum was then recorded. Chloroethylene carbonate, (20 μL, 0.245 mmol) was added next and ^{1}H NMR spectra were recorded at 5-min intervals for 30 min. There was no change in the resonances due to the trimethylbenzimidazole, with the exception of a slight downfield shift in the peak at 7.98 ppm (assigned to the B2 proton; the shift of this proton should be very sensitive to either alkylation or protonation of the N3 nitrogen). On the basis of the fact that the peak remained a singlet (as opposed to splitting into product and starting material peaks), and on the results of the second experiment below, we interpreted these spectra as indicative of no alkylation reaction over the 30-min period monitored. Given the fact that the reaction mixture was ~2.7 times as concentrated as the synthetic reaction being modeled and the time scale 6 times as long (30 min as opposed to 5 min for the synthesis of α-**1**), this experiment is evidence that the relay mechanism is not kinetically competent and can be ruled out.

In the second trial, the amount of chloroethylene carbonate was increased to 91 μL (1.11 mmol), all other factors remaining the same. Spectra were recorded prior to the addition of chloroethylene carbonate and then at 5-min intervals for 30 min. The B2 proton showed a gradual shift from 7.97 to 8.77 ppm, while the B4 and B7 resonances (7.37 and 7.25 ppm, respectively) gradually converged to a singlet at 7.51 ppm. These shifts are indicative of either an alkylation reaction at N3 or, we believe more likely, a gradual increase in the acidity of the solution resulting from base consumption by the reaction of CD_3OD (i.e., CD_3O^-) with the carbonate group in ethylene carbonate. (Alkylation seems unlikely given that two sets of peaks, corresponding to starting material and product, are not visible. Rather, the peaks gradually shift, indicating a rapid and reversible change on the NMR time scale such as protonation, resulting in an averaging of the shift values of the two states). This reaction was not pursued further, as it is slow relative to even a 6-fold longer time scale than used for the synthesis of α-**1**.

Acknowledgment. Financial support from the NIH (Grant DK-26214 at Oregon; Grant GM-29225 at Emory) is gratefully acknowledged.

Registry No. 1 (isomer 1), 132854-67-2; **1** (isomer 2), 132956-62-8; **2** (isomer 1), 132956-61-7; **2** (isomer 2), 132956-63-9; $H_2OB_{12}^+Cl^-$, 27085-12-7; pyridine, 110-86-1; 1-methylimidazole, 616-47-7; DL-histidine, 4998-57-6; chloroethylene carbonate, 3967-54-2; 1,5,6-trimethylbenzimidazole, 1128-27-4.

Supplementary Material Available: Figure A, FAB-MS spectra of the alkylcobalamins **1** and **2** with *m*-nitrobenzyl alcohol as matrix; Figure B, FT-IR spectroscopy of **1** and **2** (KBr pellet); Figure C, UV–visible spectra of **1** in deionized H_2O and of base-off **2** in 0.2 N HCl; Figure D, UV–visible spectra of **1** in 50% H_2O/50% 1-methylimidazole (v/v) and of base-on **2** in deionized H_2O; Figure E, longer mixing time (105.9 ms) 2-D HOHAHA spectrum of α_1-**1** at 500 MHz; Figure F, part of the ^{1}H-detected ^{1}H–^{13}C shift correlation (HMQC) spectrum of α_1-**1**; Figure G, part of the ^{1}H-detected ^{1}H–^{13}C multiple-bond shift correlation (HMBC) spectrum showing the ^{1}H–^{13}C correlations of the benzimidazole protons to the nonprotonated benzimidazole carbons; Figure H, 1-D ^{1}H NMR of **1** in acidic (0.7 M DCl) D_2O; Figure I, 1-D ^{1}H NMR OF **2** in acidic (0.07 M DCl) D_2O; Figure J, axial base pK_a(apparent) titrations in D_2O for α_1-**1** and α_2-**1**; further discussion of the factors (i–iii)[36a] influencing the observed ^{1}H NMR chemical shifts (13 pages). Ordering information is given on any current masthead page.